AMERICAN SOCIETY FOR MICROBIOLOGY | Journal of Virology®

VACCINES AND ANTIVIRAL AGENTS

A Temperature-Dependent Translation Defect Caused by Internal Ribosome Entry Site Mutation Attenuates Foot-and-Mouth Disease Virus: Implications for Rational Vaccine Design

Decheng Yang,[a] Chao Sun,[a] Rongyuan Gao,[a] Haiwei Wang,[a] Wenming Liu,[a] Kewei Yu,[a] Guohui Zhou,[a] Bo Zhao,[a] Li Yu[a]

[a]Division of Livestock Infectious Diseases, State Key Laboratory of Veterinary Biotechnology, Harbin Veterinary Research Institute, Chinese Academy of Agricultural Sciences, Harbin, China

Decheng Yang and Chao Sun contributed equally to this work. Author order was determined by funding sources.

ABSTRACT Foot-and-mouth disease (FMD), which is caused by FMD virus (FMDV), remains a major plague among cloven-hoofed animals worldwide, and its outbreak often has disastrous socioeconomic consequences. A live-attenuated FMDV vaccine will greatly facilitate the global control and eradication of FMD, but a safe and effective attenuated FMDV vaccine has not yet been successfully developed. Here, we found that the internal ribosome entry site (IRES) element in the viral genome is a critical virulence determinant of FMDV, and a nucleotide substitution of cytosine (C) for guanine (G) at position 351 of the IRES endows FMDV with temperature-sensitive and attenuation (*ts&att*) phenotypes. Furthermore, we demonstrated that the C351G mutation of IRES causes a temperature-dependent translation defect by impairing its binding to cellular pyrimidine tract-binding protein (PTB), resulting in the *ts&att* phenotypes of FMDV. Natural hosts inoculated with viruses carrying the IRES C351G mutation showed no clinical signs, viremia, virus excretion, or viral transmission but still produced a potent neutralizing antibody response that provided complete protection. Importantly, the IRES C351G mutation is a universal determinant of the *ts&att* phenotypes of different FMDV strains, and the C351G mutant was incapable of reversion to virulence during *in vitro* and *in vivo* passages. Collectively, our findings suggested that manipulation of the IRES, especially its C351G mutation, may serve as a feasible strategy to develop live-attenuated FMDV vaccines.

IMPORTANCE The World Organization for Animal Health has called for global control and eradication of foot-and-mouth disease (FMD), the most economically and socially devastating disease affecting animal husbandry worldwide. Live-attenuated vaccines are considered the most effective strategy for prevention, control, and eradication of infectious diseases due to their capacity to induce potent and long-lasting protective immunity. However, efforts to develop FMD virus (FMDV) live-attenuated vaccines have achieved only limited success. Here, by structure-function study of the FMDV internal ribosome entry site (IRES), we find that the C351 mutation of the IRES confers FMDV with an ideal temperature-sensitive attenuation phenotype by decreasing its interaction with cellular pyrimidine tract-binding protein (PTB) to cause IRES-mediated temperature-dependent translation defects. The temperature-sensitive attenuated strains generated by manipulation of the IRES address the challenges of FMDV attenuation differences among various livestock species and immunogenicity maintenance encountered previously, and this strategy can be applied to other viruses with an IRES to rationally design and develop live-attenuated vaccines.

KEYWORDS Foot-and-mouth disease virus, cellular PTB protein, internal ribosome

Citation Yang D, Sun C, Gao R, Wang H, Liu W, Yu K, Zhou G, Zhao B, Yu L. 2020. A temperature-dependent translation defect caused by internal ribosome entry site mutation attenuates foot-and-mouth disease virus: implications for rational vaccine design. J Virol 94:e00990-20. https://doi.org/10.1128/JVI.00990-20.

Editor Susana López, Instituto de Biotecnologia/UNAM

Address correspondence to Li Yu, yuli02@caas.cn.

Received 19 May 2020
Accepted 27 May 2020
Accepted manuscript posted online 3 June 2020
Published 30 July 2020

entry site, rational design of live-attenuated vaccine, virulence attenuation, virus-host interaction

Foot-and-mouth disease (FMD) caused by foot-and-mouth disease virus (FMDV) is the most contagious disease affecting domestic and wild cloven-hoofed animals, including pigs, cattle, sheep, and goats (1). The disease, which is widely endemic in a number of developing countries and poses a constant threat to developed countries, has a substantial effect on world agriculture not only in livestock health and production but also in international trade. Vaccination is the most economical and effective way to prevent infectious diseases. The current inactivated whole-virus vaccine to control FMD is effective in reducing the number of outbreaks worldwide, but global control of FMD is challenging because some obvious shortcomings are associated with this inactivated vaccine, including the potential escape of virulent viruses from production facilities, the short duration of immunity, the short shelf life of the formulated product, and the requirement for dozens of antigens to circumvent viral antigenic diversity (2). Thus, developing a new generation of FMDV vaccines for global control and eradication of FMD is an urgent task.

In the past 60 years, a number of alternative approaches to FMD vaccine development have been adopted (2, 3), one of which is the development of a live-attenuated vaccine. A vaccine based on stably attenuated FMDV may present better biosafety profiles for production, increase protection periods through better immune responses, and reduce the cost to promote its application. Historically, by using attenuated viral vaccines, smallpox and rinderpest viruses have been eradicated (4, 5), poliomyelitis has been nearly eradicated (6), and measles has been eliminated from some parts of the world (7). Initially, for FMDV, researchers attempted to develop live-attenuated FMDV vaccines by passage in alternate hosts and/or in tissue culture (8, 9), but obtaining viruses that are both attenuated and immunogenic has been difficult. Worse still, some immunogenic viruses were attenuated in one host but were pathogenic in another (2). Thus, research on live FMD vaccines relying on conventional empirical attenuation has not been pursued for many years.

In the past 25 years, some FMDV attenuated strains have been rationally constructed using modern biotechnology through deletion (10), insertion (11), or mutation (12, 13) of the leader proteinase (L^{pro}), partial deletion of the nonstructural protein 3A (14), and the generation of RNA-dependent RNA polymerase (RdRp) mutants with altered replication fidelity (15–17). Through functional genomics analyses, a few virulence factors of FMDV, such as L^{pro}, protein 3A, and RdRp, have been identified, and L^{pro} is the most thoroughly investigated factor. However, the attenuated virus strains obtained through these attempts have shown limited success owing equally to differences in attenuation among various livestock species (e.g., attenuated in cattle but not in swine or vice versa) or an inability to consistently induce protective immune responses after attenuation (3). Thus, developing ideally attenuated FMDV vaccine candidates will require a better understanding of the critical FMDV virulence determinant and its interaction with the host to address concerns regarding attenuated strains related to complete attenuation in all susceptible species and retention of immunogenicity.

FMDV, a member of the genus *Aphthovirus* within the family *Picornaviridae*, has seven distinct serotypes (O, A, C, Asia1, South African Territories [SAT] 1, SAT2, and SAT3) as well as multiple subtypes, and its genome consists of a single-stranded positive-sense RNA with a length of approximately 8.5 kb (1). In picornaviruses, including FMDV, the genomic 5′ untranslated regions contain an internal ribosome entry site (IRES), which facilitates translation initiation of the viral open reading frames in a cap-independent manner (18). IRES-driven translation initiation depends on the structural organization of the IRES and its interaction with cellular proteins, including translation initiation factors (eIFs) and other noncanonical translation factors termed IRES *trans*-acting factors (ITAFs) (18). The most commonly found eIF and ITAF for picornavirus IRES activity are eIF4G (19, 20) and pyrimidine tract-binding protein (PTB),

respectively (21, 22). Since the discovery of the IRES, regulation of IRES-dependent translation has been regarded as a critical step for some viral infections, with important effects on viral virulence, tissue tropism, and pathogenicity (23, 24).

This study was initiated to investigate the effect of the IRES element on the virulence of FMDV. We first found a critical virulence determinant of FMDV at domain 4 of the IRES through replacement of the FMDV IRES domain with its counterpart from bovine rhinitis B virus (BRBV). By dissecting IRES domain 4 of FMDV and BRBV, we further found that a single nucleotide substitution of cytosine (C) for guanine (G) at position 351 of the IRES endows FMDV with temperature-sensitive and attenuation (*ts&att*) phenotypes, leading to the generation of highly attenuated and immunoprotective mutants. More importantly, we elucidated the molecular mechanism for the generation of FMDV *ts&att* phenotypes, finding that the C351G mutation of IRES leads to a temperature-dependent translation defect by impairing the IRES's binding to the cellular PTB protein, resulting in the *ts&att* phenotypes of FMDV. These results demonstrated that the IRES is a critical virulence determinant of FMDV and that the C351G mutation in a PTB-binding site of the IRES can be used to construct attenuated strains for the development of potential live-attenuated FMDV vaccines.

RESULTS

Replacement of FMDV IRES domain 4 with BRBV IRES domain 4 results in attenuation of FMDV. Previously constructed IRES domain-chimeric FMDV mutants, including FMDV(R2), FMDV(R3), FMDV(R4), FMDV(R5), FMDV(RM), and FMDV(BRBV) (25), were used to investigate the effect of IRES domains on FMDV virulence (Fig. 1A). In pathogenicity tests using suckling mice, FMDV(R2), FMDV(R3), FMDV(R5), FMDV(RM), and FMDV(BRBV) showed similar virulence (50% lethal dose [LD_{50}], 0.10 to 0.42 50% tissue culture infective dose [$TCID_{50}$]) to that of the wild-type virus FMDV(WT) (LD_{50}, 0.16 $TCID_{50}$), whereas the IRES domain 4-chimeric mutant FMDV(R4) exhibited a 157-fold reduction in virulence (LD_{50}, 25.12 $TCID_{50}$) compared to that of FMDV(WT), indicating that replacement of FMDV IRES domain 4 with its corresponding counterpart in BRBV endows FMDV with an attenuation (*att*) phenotype in suckling mice.

The attenuation phenotype of FMDV(R4) was then evaluated in a natural host (Fig. 1B). Three pigs were intramuscularly (i.m.) inoculated with 10^5 50% tissue culture infective dose ($TCID_{50}$) of FMDV(WT)/pig, and another group of three pigs was inoculated with a higher dose (10^6 $TCID_{50}$) of the FMDV(R4) mutant per pig. At 24 h postinoculation, two naive pigs were mixed with the three inoculated pigs of each group to induce cohabitation infection. The FMDV(WT)-inoculated pigs (numbers [no.] 15, 18, and 46) developed FMD clinical symptoms, including lesions on the feet and mouth and fever, as early as 2 days postinoculation (dpi). Additionally, viral RNA in the sera and oral/nasal secretions was detected as early as 1 dpi and peaked at 2 to 4 dpi. The pigs (no. 10 and 35) exposed by direct contact with FMDV(WT)-inoculated pigs also developed the typical disease, and the viral RNA in the samples appeared late at 3 dpi. In contrast, none of the pigs inoculated with FMDV(R4) (no. 21, 22, and 23) or the two directly contacted pigs (no. 25 and 29) developed clinical signs of FMD (vesicular lesions, viremia, or virus shedding in oral/nasal secretions). Unexpectedly, neither neutralizing antibodies nor antibodies against nonstructural protein 3ABC were positive in the FMDV(R4)-inoculated pigs and the cohabiting pigs during 21 dpi in a microneutralization assay and 3ABC indirect enzyme-linked immunosorbent assay (ELISA), indicating that the FMDV(R4) did not replicate in the inoculated pigs. These results demonstrated that the replacement of IRES domain 4 in the FMDV genome with its BRBV counterpart leads to complete loss of FMDV infectivity in a natural host.

Replacement of IRES domain 4 endows FMDV with a significant temperature-sensitive phenotype. Since BRBV grows in the upper respiratory tract epithelium and the virus-infected cells incubated at 33°C display a more pronounced cytopathic effect (CPE) than those incubated at 37°C (26), we reasoned that BRBV is a natural temperature-sensitive (*ts*) strain, and that the FMDV(R4) mutant carrying the IRES domain 4 of BRBV may therefore be an attenuated mutant with a *ts* phenotype. To test

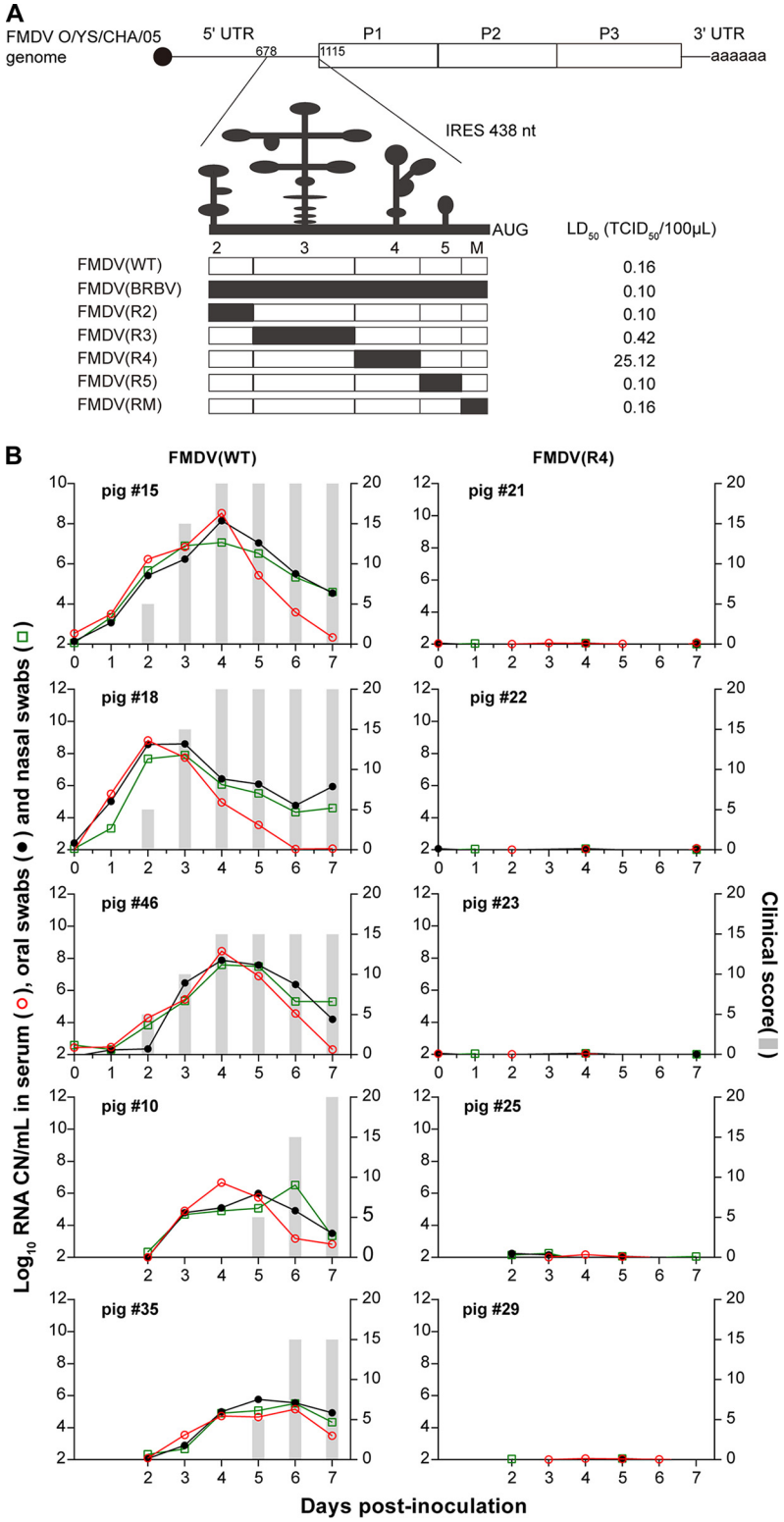

FIG 1 The virulence of chimeric-IRES FMDV mutants. (A) Schematic representation of the chimeric-IRES FMDV mutants and their virulence in suckling mice. Different groups of 3-day-old suckling mice were cervicodorsally inoculated with chimeric-IRES FMDV mutants or FMDV(WT) diluted to different titers of $TCID_{50}$. Animal deaths were scored for up to 7 days after inoculation. (B) The virulence of the mutant FMDV(R4) in pigs. Clinical signs were indicated as clinical scores, and virus yields (log_{10} of viral RNA copies/ml) in sera and oral/nasal swabs were determined daily. Viral RNA levels in serum (○) and oral (●) and nasal (□) swab samples are expressed on the left axes, and clinical scores (bars) are expressed on the right axes.

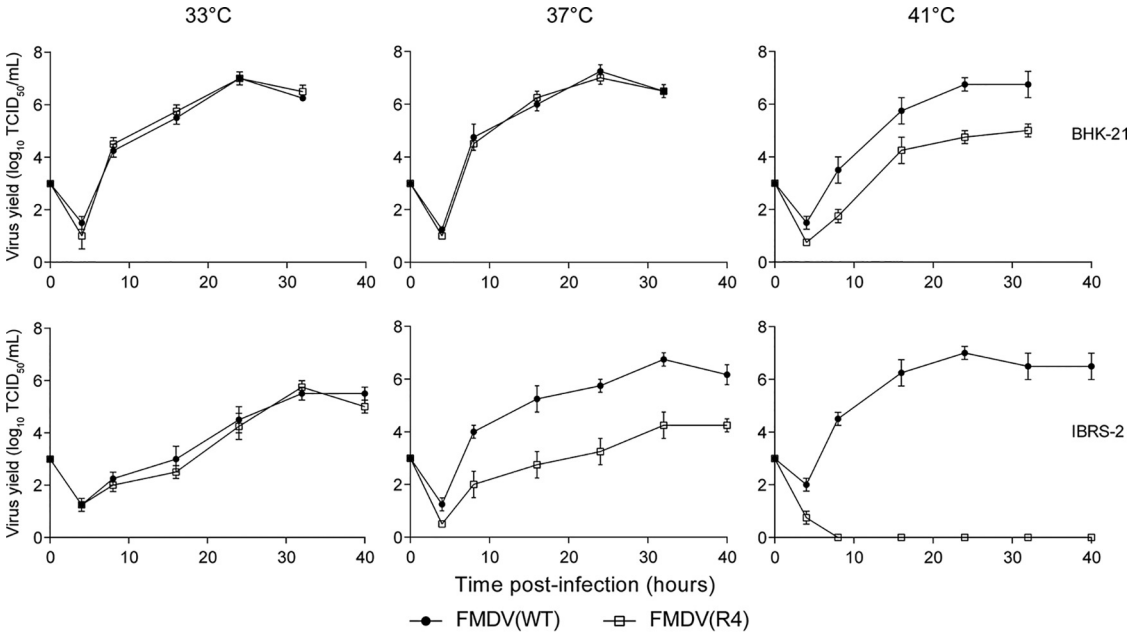

FIG 2 Growth curves of FMDV(R4) at different temperatures. The graphs indicate the growth kinetics of FMDV(WT) and FMDV(R4) in BHK-21 and IBRS-2 cells. Cells were infected and incubated at 33°C, 37°C, or 41°C. The virus titers were determined by $TCID_{50}$ assay on monolayers of BHK-21 cells. All data are expressed as the means ± standard deviations (SDs) from three independent experiments.

this hypothesis, the growth phenotypes of FMDV(R4) in BHK-21 and IBRS-2 cells were analyzed at 33°C, 37°C, and 41°C (Fig. 2). In hamster-derived BHK-21 cells, FMDV(R4) replicated with growth kinetics similar to those of FMDV(WT) at 33°C and 37°C but exhibited approximately 10-fold lower growth kinetics than those of FMDV(WT) at 41°C at the peak of viral replication, reflecting a mild *ts* phenotype. In porcine-derived IBRS-2 cells, the multiplication of FMDV(R4) was more significantly inhibited by increased temperature, as its viral titer decreased approximately 1,000-fold at 37°C and its replication was eventually completely restricted at 41°C (Fig. 2). These results confirmed our hypothesis that replacement of IRES domain 4 confers FMDV with a *ts* phenotype. In addition, the *ts* phenotype of FMDV(R4) was more obvious in the IBRS-2 cells derived from susceptible host pigs than in the hamster-derived BHK-21 cells.

The nucleotide cytosine at position 351 of the IRES determines the *ts&att* phenotypes of FMDV. To identify the genetic determinant(s) responsible for the *ts&att* phenotypes of FMDV, IRES domain 4 was dissected functionally according to its secondary structure. First, three IRES subdomain-chimeric FMDV mutants (designated rdJ, rdK, and rdN) were constructed (Fig. 3A) by replacing each subdomain of FMDV IRES domain 4 with its BRBV counterpart, and their growth phenotypes were analyzed. As shown in Fig. 4A and B, the replication kinetics of rdJ and rdN were similar to those of FMDV(WT), whereas the chimera rdK showed a *ts* phenotype similar to that of FMDV(R4). Subsequently, the virulence of rdK, rdJ, and rdN was evaluated in suckling mice. As anticipated from the growth properties in cultured cells, the IRES chimeras rdJ and rdN presented an LD_{50} (0.10 to 0.24 $TCID_{50}$) similar to that (LD_{50}, 0.16 $TCID_{50}$) of FMDV(WT), while the chimera rdK exhibited a 10^4-fold reduction in virulence (LD_{50}, 1585 $TCID_{50}$) (Fig. 3A). These results indicated that substitution of subdomain K from the BRBV IRES determines the *ts&att* phenotypes of FMDV(R4).

To further define the portion of IRES subdomain K responsible for the *ts&att* phenotypes of FMDV, two more precise IRES-chimeric mutants, rK(stem) and rK(loop), were constructed by replacing the stem and loop of FMDV IRES subdomain K, respectively, with those of BRBV IRES subdomain K (Fig. 3B). As shown in Fig. 4C and D, rK(stem) exhibited a growth profile similar to that of FMDV(WT), whereas rK(loop) replicated with growth kinetics similar to those of FMDV(R4), indicating that substitu-

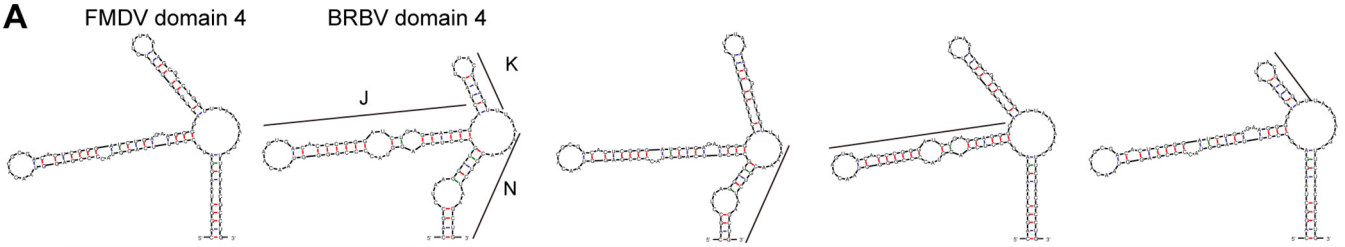

Virus	rdN	rdJ	rdK
LD50 (TCID50/100μL)	0.24	0.10	1585

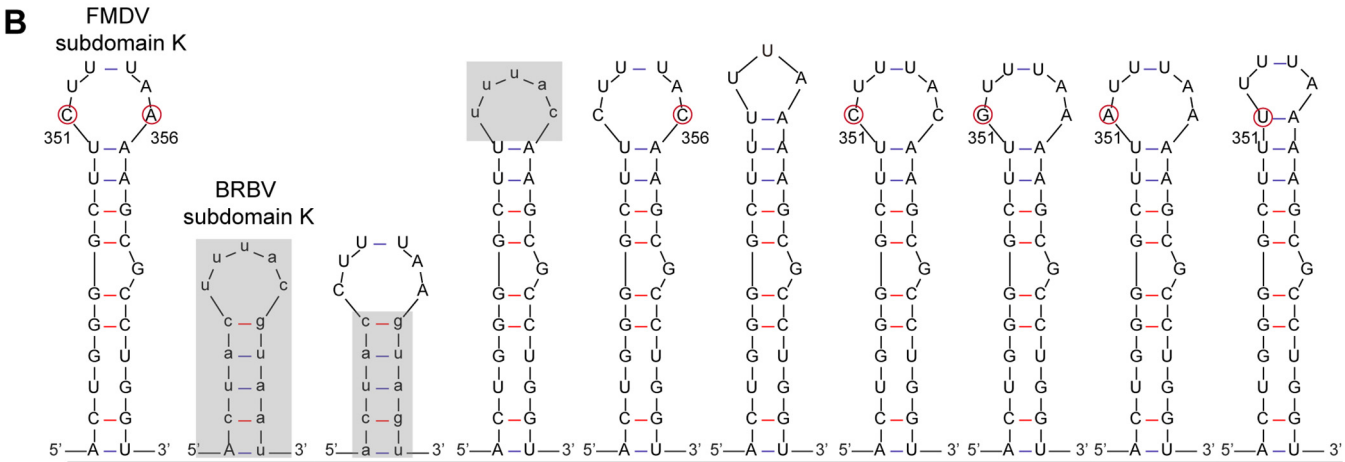

Virus	rK(Stem)	rK(Loop)	rA356C	rDel-C351	rIns-C351	rC351G	rC351A	rC351U
LD50 (TCID50/100μL)	0.15	0.10	0.10	——	0.06	1585	316	——

FIG 3 Schematic representations of the chimeric-IRES and IRES-mutated FMDV mutants and their virulence in suckling mice. The secondary structure of each chimeric and mutated IRES construct was predicted using mfold software (version 3.6). The portal for the mfold web server is http://www.bioinfo.rpi.edu/applications/mfold (47). Different groups of suckling mice were cervicodorsally inoculated with IRES mutants or FMDV(WT) at different $TCID_{50}$ titers. Animal deaths were scored for up to 7 days after inoculation.

tion of the loop region in subdomain K from the BRBV IRES is responsible for the *ts* phenotype of FMDV(R4).

Unexpectedly, no attenuation was observed for rK(loop) in suckling mice (LD_{50}, 0.10 $TCID_{50}$), as shown in Fig. 3B, in contrast to the *ts* phenotype of this chimera in BHK-21 cells and IBRS-2 cells (Fig. 4C and D). The complete genome of the virulent virus isolated from the suckling mice that died due to inoculation with rK(loop) was sequenced, revealing that the nucleotide cytosine (C) inserted at IRES position 351 in rK(loop) lead to reversion of rK(loop) to the virulent type. These results suggested that the C at position 351 of the FMDV IRES is important for the *ts&att* phenotypes of FMDV(R4).

The loop sequence (^{351}CUUUAA^{356}) in subdomain K of the FMDV IRES is similar to the corresponding sequence (UUUAC) in BRBV but has an extra C at position 351 and one nucleotide difference at position 356 (Fig. 3B). To test which nucleotide in the loop determined the *ts&att* phenotypes of FMDV, single-nucleotide mutations, deletions, or insertions were introduced into the loop (^{351}CUUUAA^{356}) of FMDV (Fig. 3B). First, the A356C mutation was introduced in the loop (^{351}CUUUAA^{356}), and the rescued mutant rA356C with a modified loop ^{351}CUUUAC^{356} did not show a *ts* phenotype (Fig. 4E and F) or an *att* phenotype (Fig. 3B), indicating that the nucleotide difference at the position of 356 in the loop of IRES subdomain K is not related to the viral *ts&att* phenotypes. Thus, we focused on another difference in the loop sequence (^{351}CUUUAA^{356}) of the FMDV IRES—an extra C at position 351. To verify the role of IRES C351 in the generation of viral *ts&att* phenotypes, we first constructed an infectious clone with an IRES C351

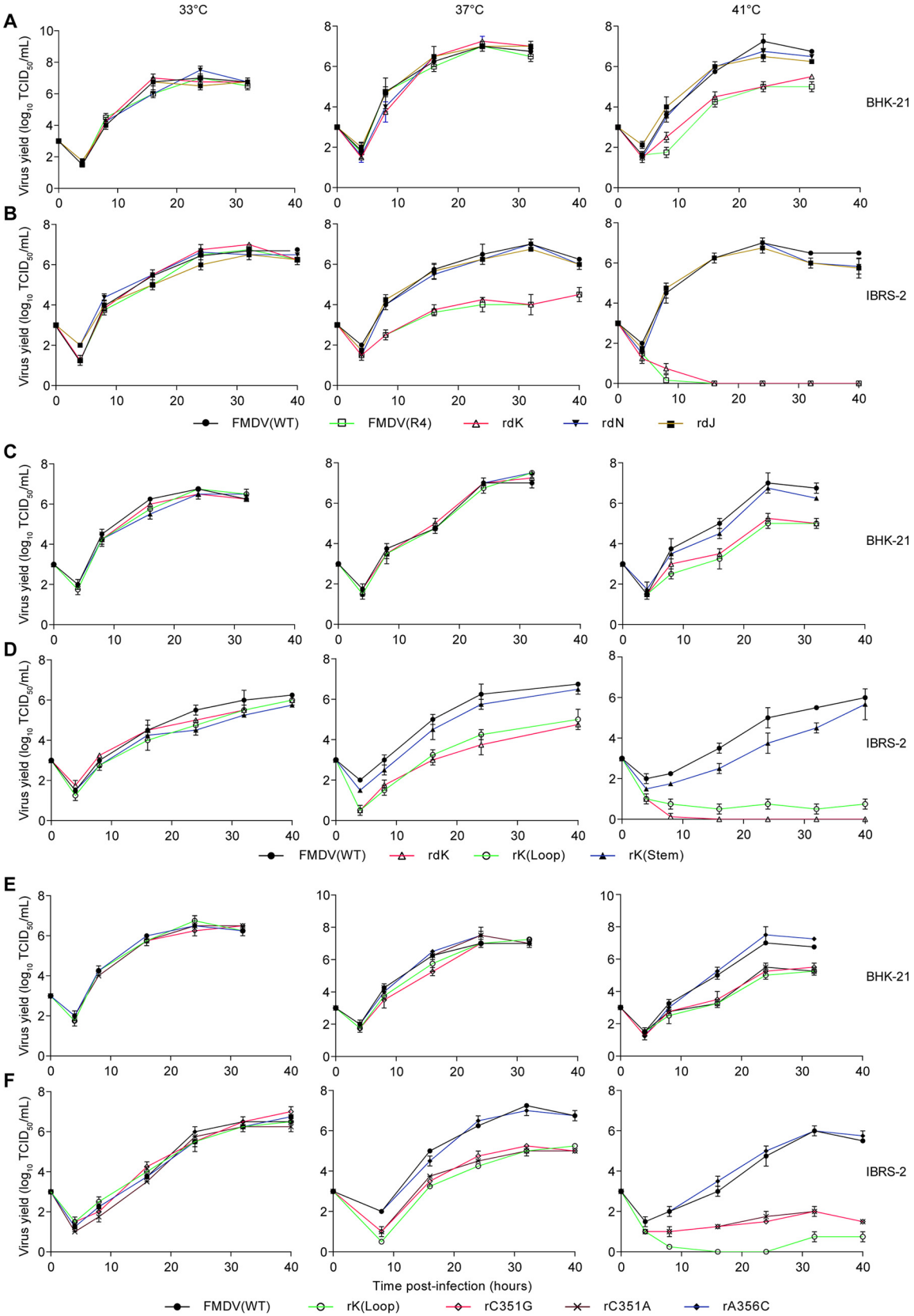

FIG 4 Growth curves of the FMDV mutants. The graphs indicate the growth kinetics of the chimeric-subdomain IRES mutants (A and B), IRES chimeric-stem or chimeric-loop mutants (C and D), and C351-mutated IRES mutants (E and F) in BHK-21 and IBRS-2 cells. Cells were infected at an MOI of 0.05 and incubated at 33°C, 37°C, or 41°C. Virus titers were determined by $TCID_{50}$ assay on monolayers of BHK-21 cells. All data are expressed as the means ± SDs from three independent experiments.

deletion in the backbone of FMDV(WT) to rescue rDel-C351, finding that the C351 deletion was lethal for FMDV replication (Fig. 3B). Subsequently, we generated the reverse mutant, rIns-C351, in which the loop ^{351}UUUAC^{355} of subdomain K in the BRBV IRES was changed into ^{351}CUUUAC^{356} by insertion of a C at the 350/351 position in the background of the rK(loop) genome. The rescued virus rIns-C351, which is simply the rA356C mutant as indicated in Fig. 3B, also lost its *ts* and *att* phenotypes as shown in Fig. 4E and F and Fig. 3B, providing evidence that the absence of C351 in the IRES of rK(loop) contributed to the *ts&att* phenotypes of rK(loop). These results indicated that the nucleotide cytosine (C) at position 351 in the loop of subdomain K of the FMDV IRES is important for the *ts&att* phenotypes of FMDV. Since the nucleotide C351 deletion is lethal for viral replication, we constructed three FMDV mutant infectious clones through C351G, C351A, or C351U substitution (Fig. 3B). After transfection, the mutants rC351G and rC351A were rescued, whereas the C351U mutation was lethal for FMDV. Importantly, the replication ability of rC351A and rC351G, similar to that of FMDV(R4), significantly decreased in BHK-21 cells at 41°C (Fig. 4E) and in IBRS-2 cells at 37°C and 41°C (Fig. 4F). In addition, the LD_{50}s of rC351G and rC351A decreased approximately 10^4-fold and 2×10^3-fold, respectively, in suckling mice (Fig. 3B).

Through chimerization of IRES domain 4 and its subdomains and mutagenesis of the loop (^{351}CUUUAA^{356}) in subdomain K of FMDV IRES domain 4, our results demonstrated that the nucleotide C351 in the loop of IRES subdomain K is the determinant for the *ts&att* phenotypes of FMDV.

The FMDV *ts&att* phenotypes caused by the C351G mutation of IRES are the result of a temperature-dependent translation defect. Given that rC351G was more attenuated than rC351A in suckling mice, rC351G was selected to explore the molecular mechanism for the generation of its *ts&att* phenotypes. First, two dual-luciferase reporters, pCMV-RHF-IRES(WT) and pCMV-RHF-IRES(C351G), were constructed using the IRES elements from FMDV(WT) or rC351G, and their IRES-mediated translation capacity was assessed by measuring the yield ratio of firefly luciferase (FLuc) expression to *Renilla* luciferase (RLuc) expression at 24 h posttransfection (Fig. 5A). In BHK-21 cells, a significant reduction in IRES activity for rC351G was observed at 41°C compared to that at 33°C or 37°C (Fig. 5A). In the pig-derived IBRS-2 cells, the IRES activity of rC351G was increasingly restrained with an increasing temperature from 33°C to 37°C, and the IRES almost lost its ability to initiate translation at 41°C (Fig. 5A). These results indicated that the C351G mutation of the IRES leads to a temperature-dependent translation defect in BHK-21 cells and more significant temperature-dependent translation defects in IBRS-2 cells.

Furthermore, the kinetics of viral gene expression and titers of virus production were analyzed to evaluate the effect of the IRES C351G mutation on replication of the mutant rC351G in infected BHK-21 and IBRS-2 cells. As shown in Fig. 5B, the expression of viral VP2 protein gradually decreased with increasing temperatures in these rC351G-infected cells and even reached very low levels in the rC351G-infected IBRS-2 cells at 41°C, which was consistent with the trend of decreasing infectious virus titers with increasing temperature (Fig. 5C). These results supported that the C351G mutation of the IRES leads to temperature-dependent translation defects at the levels of viral protein synthesis and viral particle production.

Thus, we concluded that the C351G mutation of the IRES causes a temperature-dependent translation defect in rC351G-infected cells, which endows FMDV with *ts&att* phenotypes.

The temperature-dependent IRES translation defect caused by the C351G mutation is mediated by the cellular PTB protein. The cap-independent translation initiation mediated by IRESs requires cellular ITAFs. A commonly found ITAF interacting with picornavirus IRES elements is PTB (27), and one of its binding motifs in the FMDV IRES is ^{351}CUUUA^{355} in the apical loop of subdomain K of FMDV IRES domain 4 (28, 29). Since the C351G mutation in this loop of IRES was determined to be responsible for the temperature-dependent translation defect of FMDV mutant rC351G (Fig. 5), we reasoned that a critical role of PTB may be related to the temperature-dependent trans-

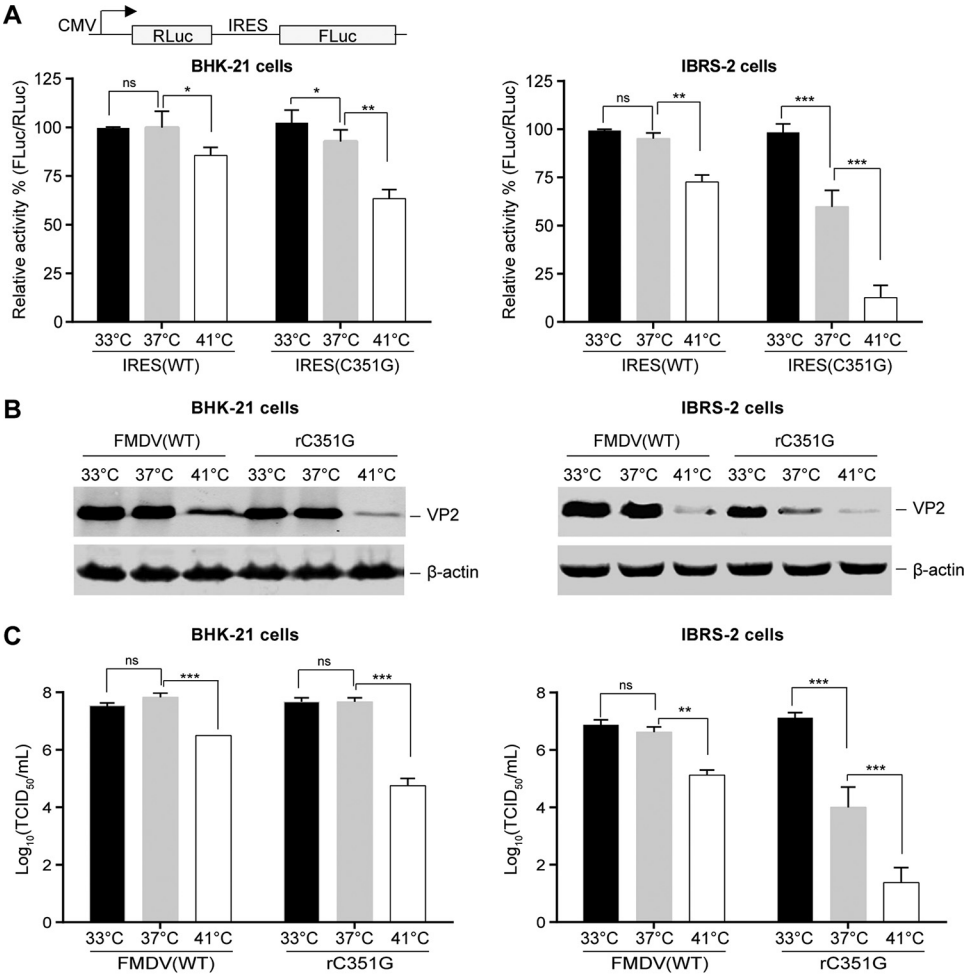

FIG 5 IRES-directed translation initiation efficiency. Monolayers of BHK-21 or IBRS-2 cells were transfected with the dual-luciferase reporter pCMV-RHF-IRES(WT) or pCMV-RHF-IRES(C351G), respectively. (A) IRES-directed translation initiation efficiency was assessed by measuring the yield ratio of FLuc expression to RLuc expression at 24 h posttransfection. BHK-21 or IBRS-2 cells were infected with rC351G or FMDV(WT) at 33°C, 37°C, or 41°C, and the resulting virus was harvested at 24 h and analyzed for VP2 protein expression by Western blotting (B) and for virus titer detection by $TCID_{50}$ assay (C). The mean values ± standard deviations are shown ($n = 3$). ns, $P > 0.05$; *, $P < 0.05$; **, $P < 0.01$; ***, $P < 0.001$ (determined by two-way analysis of variance [ANOVA] test followed by Bonferroni's *post hoc* analysis).

lation defect caused by the C351G mutation. To investigate this hypothesis, we detected the ability of the C351G IRES to bind to PTB using a biotinylated RNA-protein pulldown assay (Fig. 6A), finding that compared with that of the wild-type IRES, the C351G mutation impaired the binding of IRES to PTB. Importantly, the binding of PTB to the IRES was increasingly restrained when the temperature increased from 37°C to 41°C (Fig. 6A). To provide accurate affinity measurements of the C351G IRES-PTB interaction in FMDV attenuation, their equilibrium dissociation constants (K_D) were quantitatively detected by using biolayer interferometry. The results revealed that compared to that of the wild-type IRES, the IRES with the C351G mutation showed a reduced binding affinity to PTB with increasing temperature by 1.22-fold at 33°C, 1.37-fold at 37°C, and 4.62-fold at 41°C (Fig. 6B), further supporting that the C351G mutation impaired the interaction of the FMDV IRES with the cellular PTB in a temperature-dependent manner.

To determine whether impaired IRES-PTB binding correlates with the IRES-mediated temperature-dependent translation defect, an IBRS-2 cell line stably overexpressing PTB (IBRS-2^{PTB}) was generated (Fig. 6C). In IBRS-2^{PTB} cells, the IRES activity of rC351G was significantly enhanced at 37°C and 41°C compared to that in the IBRS-$2^{ZsGreen}$ cells

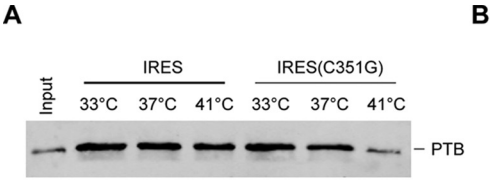

B

	Temperature	K_D (M)	K_{on} (1/Ms)	K_{dis} (1/s)
IRES/PTB	33℃	3.18E-08	6.27E+04	1.99E-03
	37℃	5.84E-08	4.89E+04	2.85E-03
	41℃	1.41E-07	4.14E+04	5.83E-03
IRES(C351G)/PTB	33℃	3.88E-08	5.77E+04	2.24E-03
	37℃	8.03E-08	4.61E+04	3.70E-03
	41℃	6.51E-07	2.15E+04	1.40E-02

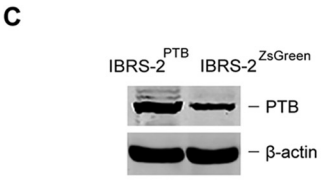

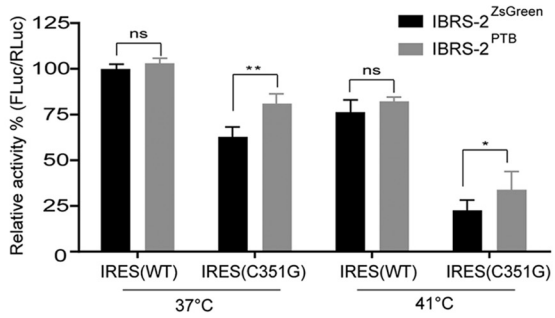

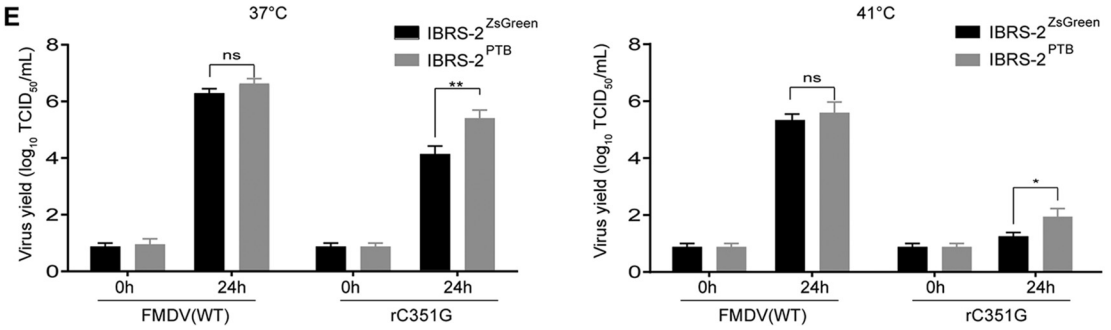

FIG 6 C351G mutation impairment of the binding of IRES with PTB in a temperature-dependent manner. (A) In an RNA pulldown assay, biotinylated IRES or its C351G mutant was incubated with PTB purified from *E. coli* for Western blot analysis. (B) Binding affinity of the FMDV IRES and its C351G mutant to PTB. (C) PTB expression in cell lines is shown using anti-PTB antibodies, and β-actin was included as a loading control. (D) The effect of PTB overexpression on IRES-mediated translation efficiency. Monolayers of cells were transfected with the dual-luciferase reporters pCMV-RHF-IRES(WT) and pCMV-RHF-IRES(C351G), and the IRES-directed translation efficiency was assessed by measuring the yield ratio of FLuc expression to RLuc expression at 24 h posttransfection. (E) The titers of rescued viruses were determined by $TCID_{50}$ assay. The mean values $\pm$ standard deviations are shown ($n = 3$). ns, $P > 0.05$; *, $P < 0.05$; **, $P < 0.01$ (determined by two-way ANOVA test followed by Bonferroni's *post hoc* analysis).

serving as controls, whereas the IRES activity of FMDV(WT) as a viral IRES control showed no apparent increase (Fig. 6D). Furthermore, the restricted growth phenotype of rC351G was significantly rescued, and the stimulatory effect of PTB overexpression on the production of rC351G was significantly enhanced in IBRS-2^{PTB} cells at 37°C and 41°C (Fig. 6E). These results indicated that overexpression of PTB in IBRS-2 cells significantly overcomes the observed temperature-dependent translation defect caused by the IRES C351G mutation and also the growth defect of rC351G, further confirming that the impaired binding of the mutated IRES to PTB correlates with the IRES-mediated temperature-dependent translation defect.

Taken together, these results indicated that the C351G mutation renders the interaction of the IRES with cellular PTB sensitive to temperature, resulting in the IRES-mediated temperature-dependent translation defect, which endows FMDV with a *ts* phenotype in cell lines and *ts&att* phenotypes in animals.

The IRES C351G mutants of FMDV are highly attenuated and induce protection against an FMDV challenge. To assess the virulence attenuation of the IRES C351G mutants of FMDV in natural hosts, pathogenicity tests were performed in pigs and cattle. Groups of three pigs were first i.m. inoculated with 10^5 $TCID_{50}$ of FMDV(WT) or

TABLE 1 Responses of animals inoculated with IRES C351G mutants

Inoculum and dose	Route of exposure	Animal no.	Maximum clinical score (dpi)[a]	Maximum viral RNA copies/ml (dpi)[b]			3ABC antibody[c]	NT_{50}[d]	
				Serum	Oral swab	Nasal swab		7 dpi	14 dpi
FMDV(WT) 1×10^5 $TCID_{50}$/pig	Direct	Pig 11	20 (4)	6.9×10^9 (3)	1.4×10^8 (3)	3.9×10^8 (3)	Pos.	64	256
	Direct	Pig 12	18 (4)	1.4×10^8 (4)	7.7×10^8 (4)	3.1×10^8 (4)	Pos.	32	256
	Direct	Pig 13	20 (3)	3.3×10^{10} (3)	4.0×10^8 (3)	2.3×10^8 (3)	Pos.	64	128
	Contact	Pig 16	14 (6)	1.4×10^7 (5)	5.8×10^5 (5)	2.4×10^5 (6)	Pos.	8	128
	Contact	Pig 19	12 (6)	1.4×10^8 (5)	5.8×10^6 (5)	6.5×10^6 (5)	Pos.	<8	64
rC351G 1×10^6 $TCID_{50}$/pig	Direct	Pig 36	0	Neg.[c]	Neg.	Neg.	Pos.	<8	64
	Direct	Pig 49	0	Neg.	Neg.	Neg.	Pos.	64	256
	Direct	Pig 59	0	Neg.	Neg.	Neg.	Pos.	32	128
	Contact	Pig 28	0	Neg.	Neg.	Neg.	Neg.	<8	<8
	Contact	Pig 57	0	Neg.	Neg.	Neg.	Neg.	<8	<8
O01-WT 1×10^7 $TCID_{50}$/bovine	Direct	Bovine 08	16 (4)	8.8×10^7 (3)	1.1×10^7 (4)	6.9×10^6 (3)	Pos.	512	512
	Direct	Bovine 09	12 (5)	6.1×10^7 (3)	3.8×10^7 (4)	4.8×10^6 (3)	Pos.	256	256
	Direct	Bovine 10	8 (5)	8.2×10^6 (4)	6.7×10^6 (5)	5.1×10^6 (5)	Pos.	512	1,024
O01-rC351G 1×10^7 $TCID_{50}$/bovine	Direct	Bovine 04	0	Neg.	Neg.	Neg.	Pos.	64	64
	Direct	Bovine 06	0	Neg.	Neg.	Neg.	Pos.	256	256
	Direct	Bovine 07	0	Neg.	Neg.	Neg.	Pos.	256	256
	Contact	Bovine 05	0	Neg.	Neg.	Neg.	Neg.	<8	<8
	Contact	Bovine 11	0	Neg.	Neg.	Neg.	Neg.	<8	<8

[a]Clinical scores, with a maximum of 20, are based on the number of sites (eight digits, mouth, and nostrils) containing vesicular lesions. dpi, days postinoculation.
[b]Values are expressed as the peak of RNA copies/ml at the specified dpi. The RNA copy number minimum detection level was $10^{2.6}$ RNA copies/ml. Neg., negative; Pos., positive.
[c]Antibodies against the FMDV nonstructural protein 3ABC.
[d]The FMDV-specific neutralizing antibody titer (NT) was determined as the reciprocal of the last serum dilution to neutralize 100 $TCID_{50}$ of virus in 50% of the wells (NT_{50}).

with 10^6 $TCID_{50}$ of rC351G, and two naive pigs were mixed with each group to induce cohabitation infection at 24 h postinoculation (Table 1). The pigs (no. 11, 12, and 13) inoculated with FMDV(WT) developed typical FMD symptoms 2 dpi and had high clinical scores by 3 to 4 dpi. All pigs developed viremia on the day prior to the appearance of clinical signs, and the viral RNA present in sera as well as in oral/nasal swabs was detectable starting 1 dpi and peaked at 3 to 4 dpi. The pigs exposed by direct contact (no. 16 and 19) also developed the disease, albeit with a slight delay, but had lower clinical scores, and the viral RNA reached a peak at 5 dpi in sera as well as in oral/nasal swabs. In contrast, the pigs (no. 36, 49, and 59) inoculated with 10^6 $TCID_{50}$ of rC351G and the two directly contacted pigs (no. 28 and 57) showed no clinical signs of FMD, and no viral RNA was detectable in sera or in oral/nasal swabs over 7 days. These results indicated that rC351G is a highly attenuated FMDV strain that does not produce viremia and viral shedding in inoculated pigs.

All the pigs inoculated with rC351G developed high levels of FMDV-specific neutralizing antibodies starting at 7 dpi, with a peak occurring at 14 dpi (Table 1). Similarly to the FMDV(WT)-inoculated pigs, the rC351G-inoculated pigs also produced antibodies against nonstructural protein 3ABC (Table 1), an indicator of viral replication, demonstrating that rC351G replicated in the pigs. However, neither antibodies against 3ABC nor neutralizing antibodies were detected in the two contact-exposed pigs (no. 28 and 57), indicating that no virus transmission occurred from rC351G-inoculated pigs (Table 1). These data indicated that rC351G is an ideally attenuated FMDV strain that can induce strong neutralizing antibodies by replicating in pigs but does not possess a viral shedding capacity in inoculated pigs or a horizontal transmission capacity among contacted natural hosts.

To test the virulence attenuation of rC351G in cattle, a group of three bovines was first inoculated with 10^7 $TCID_{50}$ of FMDV(WT). Unexpectedly, the cattle inoculated with the wild-type virus FMDV(WT) showed no clinical FMD symptoms or viremia, and neither serum neutralizing antibodies nor antibodies against 3ABC were detected at 14 dpi by microneutralization assay and 3ABC indirect ELISA, indicating that FMDV(WT) does not infect cattle. Thus, another type O FMDV strain, O/CHA/2001 (O01-WT), a

TABLE 2 Immunoprotection of rC351G-inoculated pigs against a challenge with O/M98/CHA/2010[a]

Inoculum and dose	Pig no.	Maximum clinical score (dpc)[b]	Maximum viral RNA copies/ml (dpc)[c]			3ABC antibody[d]	NT_{50}[e]	
			Serum	Oral swab	Nasal swab		0 dpc	7 dpc
rC351G 1×10^6 $TCID_{50}$/pig	60	0	Neg.	Neg.	Neg.	Pos.	128	512
	66	0	Neg.	Neg.	Neg.	Pos.	128	512
	68	0	Neg.	Neg.	Neg.	Pos.	64	256
PBS 1 ml/pig	65	20 (4)	5.9×10^8 (3)	1.4×10^8 (3, 4)	3.4×10^8 (4)	Neg.	<8	64
	73	16 (3)	1.4×10^6 (2)	5.8×10^7 (3)	6.3×10^7 (3, 4)	Neg.	<8	45

[a]The challenge dose of O/M98/CHA/2010 was 1,000 PID_{50} per pig.
[b]Clinical scores, with a maximum of 20, are based on the number of sites containing vesicular lesions. dpc, days postchallenge.
[c]The RNA copy number minimum detection level was $10^{2.6}$ RNA copies/ml. Neg., negative; Pos., positive.
[d]Antibodies against the FMDV nonstructural protein 3ABC at 0 dpc.
[e]The FMDV-specific neutralizing antibody titer (NT) was determined as the reciprocal of the last serum dilution to neutralize 100 $TCID_{50}$ of virus in 50% of the wells (NT_{50}).

PanAsia lineage strain that is closely related to the O/CHA/99 strain and also pathogenic to cattle, was selected to construct an IRES C351G mutant, O01-rC351G, in the infectious clone of O01-WT. The O01-rC351G mutant exhibited a *ts* phenotype (data not shown) similar to that of rC351G in IBRS-2 cells (Fig. 4F) and an *att* phenotype (data not shown) similar to that of rC351G in suckling mice (Fig. 3B), indicating that the C351G mutation of the IRES is also responsible for the *ts*&*att* phenotypes of O01-rC351G. Furthermore, two groups of bovines, with three animals in each group, were inoculated with 10^7 $TCID_{50}$ of O01-WT or 10^7 $TCID_{50}$ of O01-rC351G (Table 1). As shown in Table 1, the three bovines (no. 08, 09, and 10) that received 10^7 $TCID_{50}$ of O01-WT showed clinical signs of FMD by 2 dpi and had maximum clinical scores by 4 or 5 dpi, and the viral RNA in serum and oral/nasal secretions was detectable by 3 dpi. In contrast, the three bovines (no. 04, 06, and 07) inoculated with 10^7 $TCID_{50}$ of O01-rC351G and the two directly contacted bovines (no. 05 and 11) showed no clinical signs, viremia, or viral shedding in oral/nasal secretions (Table 1). Importantly, the O01-rC351G-inoculated bovines were able to produce neutralizing antibodies that peaked at 7 to 14 dpi, and the antibodies against 3ABC were also positive, but neither serum neutralizing antibodies nor antibodies against 3ABC were detected in the two contact-exposed bovines (Table 1). These results showed that this IRES C351G mutant of FMDV is also highly attenuated in cattle and can induce strong neutralizing antibodies by replicating in cattle without viral shedding or horizontal transmission from inoculated bovines. The situation of O01-rC351G in cattle mirrors that of rC351G in pigs, indicating that FMDV strains carrying the IRES C351G mutation are highly attenuated and potently immunogenic in multiple species of host animals.

To determine the immunoprotective efficacy of the IRES C351G mutants, rC351G was selected to inoculate natural host pigs followed by a challenge with the virulent FMDV strain O/M98/CHA/2010 (1,000 pig median infected dose [PID_{50}]/animal, i.m.) at 21 dpi, and the phosphate-buffered saline (PBS)-inoculated pigs were used as controls. After the challenge, the control pigs (no. 65 and 73) developed FMD signs and lesions within 1 to 3 days postchallenge (dpc), and the viral RNA was detectable in sera and oral/nasal swab samples (Table 2). In contrast, in all the rC351G-inoculated pigs (no. 60, 66, and 68), no clinical signs were observed, and no viral RNA in sera or oral/nasal secretions was detected after the challenge (Table 2). These results showed that a single-dose rC351G vaccination was sufficient to induce rapid and complete protection against a challenge with a heterologous subtype of FMDV.

The C351G mutation is genetically stable during *in vitro* and *in vivo* passaging. One of the main concerns regarding live-attenuated vaccines is the possibility of reversion to the wild-type virus, especially for FMDV as an RNA virus with a quasispecies nature (30). To assess the phenotypic and genetic stability of the mutant carrying the C351G mutation, rC351G was serially passaged 20 times in BHK-21 cells. Viral RNA was extracted from 20th-passage (p20) stocks, and only a nucleotide mutation (C to T) was found at the 4837 position after sequencing the entire genome—an amino acid

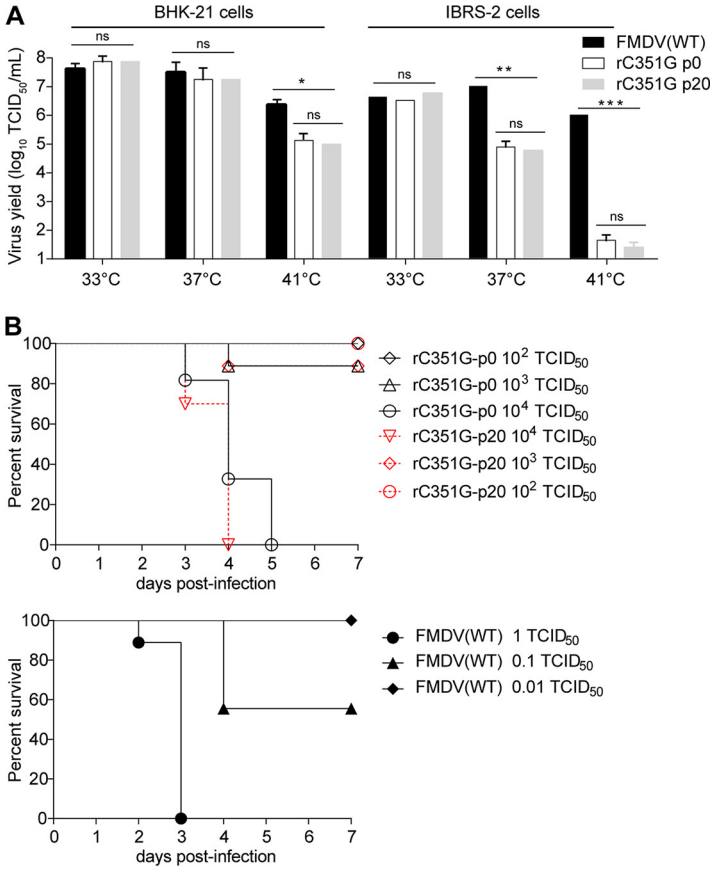

FIG 7 The stabilities of the *ts&att* phenotypes of the rC351G mutant during passaging in BHK-21 cells. (A) Twenty serial passages were performed in BHK-21 cells infected with rC351G. The 20th passage (p20) of rC351G was investigated for a *ts* phenotype in BHK-21 and IBRS-2 cells at different temperatures. The resulting virus was evaluated for titers by $TCID_{50}$ assay on BHK-21 cells. (B) The virulence of rC351G p20 was tested in suckling mice. The suckling mice were cervicodorsally inoculated with rC351G, rC351G p20, or FMDV(WT) diluted to different titers of $TCID_{50}$; animal deaths were scored for up to 7 days after inoculation, and survivors were euthanized ($n = 6$ to 9 for each group).

substitution (T135I) in nonstructural protein 2C, which is required for adaptation of the FMDV strain to BHK-21 cells as reported previously (31). The C4837T mutation also emerged in parallel passages of FMDV(WT). Importantly, the IRES C351G mutation of rC351G p20, its *ts* phenotype in cells (Fig. 7A), and its attenuation phenotype in suckling mice (Fig. 7B) remained unchanged. The nucleotide substitution was not observed at position G351 of IRES in rC351G after 20 passages, which is the genetic basis for the stable temperature-sensitive and attenuation phenotypes of the mutant rC351G observed here.

To further investigate whether the C351G mutant could revert to virulence in natural hosts, three 2-month-old pigs in one group were inoculated i.m. with 10^6 $TCID_{50}$ of rC351G, and then the tonsils, sera, and oral/nasal secretions were collected and homogenized for subsequent *in vivo* passaging of the virus in another three-pig group. The mutant rC351G was blindly passaged 3 times in the pigs, the inoculated pigs were observed daily for clinical signs, and sera and oral/nasal secretions were subjected to viral RNA detection. During the 5 days of clinical observation in each group, all animals showed no clinical signs, and no viral RNA was detected. In addition, no serum neutralizing antibodies or anti-3ABC antibodies were detected in the final three-pig group at 7 and 14 dpi. These results demonstrated that the mutant rC351G carrying the IRES C351G mutation, which does not produce viremia, viral shedding, or contact transmission in inoculated pigs or cohabitation pigs (Table 1), did not revert to virulence during *in vivo* passaging.

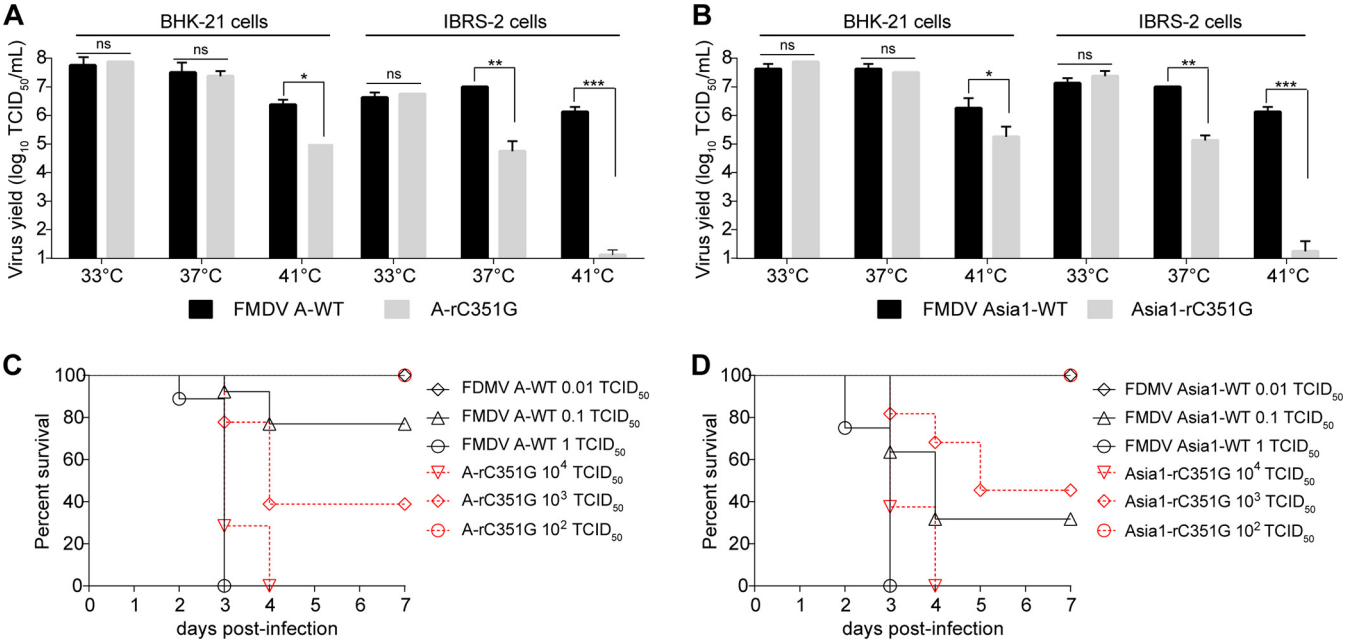

FIG 8 The IRES C351G mutation causes *ts&att* phenotypes in serotype A and serotype Asia1 FMDV. BHK-21 and IBRS-2 cells were infected with A-rC351G (A) or Asia1-rC351G (B) at different temperatures. The resulting viruses were evaluated for titers by $TCID_{50}$ assay. The virulence of A-rC351G (C) and Asia1-rC351G (D) was evaluated in suckling mice. Suckling mice were cervicodorsally inoculated with Ar-C351G, FMDV A-WT, Asia1-rC351G, or FMDV Asia1-WT diluted to different titers of $TCID_{50}$. Animal deaths were scored for up to 7 days after inoculation, and survivors were euthanized.

The *ts&att* phenotypes caused by the IRES C351G mutation are universal among different serotypes of FMDV. To investigate whether the *ts&att* phenotypes caused by the C351G mutation of the IRES are universal in different serotypes of FMDV, this mutation was introduced into the infectious clones of other serotypes of FMDV strains (Asia1/YS/CHA/05 and A/XJBC/CHA/2010), and the rescued viruses (Asia1-rC351G and A-rC351G) were examined for their *ts&att* phenotypes. As shown in Fig. 8A and B, the A-rC351G and Asia1-rC351G mutants similarly displayed a *ts* phenotype, indicating that the C351G mutation of the IRES is also responsible for the *ts* phenotype of A and Asia1 serotypes of FMDV strains. In addition, compared with that of the respective wild-type viruses in suckling mice, the A-rC351G and Asia1-rC351G mutants presented an approximately 10,000-fold virulence reduction in suckling mice, with an *att* phenotype similar to that of rC351G (Fig. 8C and D). Importantly, the PTB binding site ^{351}CUUUA^{355} in the IRES is highly conserved among distinct FMDV genomes, and the C351 nucleotide is conserved in the IRES sequences among all seven serotypes of FMDV strains available in GenBank. Considering that the temperature-dependent translation defect is caused by the IRES C351 mutation and that the IRES C351 nucleotide is absolutely conserved in all FMDV strains, the nucleotide C351 in the IRES is a universal determinant of the *ts&att* phenotypes among different serotypes of FMDV.

DISCUSSION

The main obstacle to develop live-attenuated FMDV vaccines is the difference in attenuation among different cloven-hoofed animal species (attenuated in cattle but not in swine, or attenuated in swine but not in cattle) (2, 3). Given that all cloven-hoofed animals have body temperatures higher than 37°C, we propose that FMDV temperature-sensitive mutants should be able to be attenuated among all of these animal species. FMDV usually grows normally at 37°C *in vitro* (32), while bovine rhinitis B virus BRBV, as another member of the genus *Aphthovirus* within the family *Picornaviridae*, inhabits the upper respiratory tracts of cattle and is suitable for growth at 33°C *in vitro* (26). Thus, our attenuation strategy for FMDV was to begin with swapping the domains of the IRESs between FMDV and BRBV that share similar secondary structures

(33) to explore the relatedness of the IRES stem-loop structures with virus replication at different temperatures. As expected, we obtained an attenuated IRES chimera, FMDV(R4), in which IRES domain 4 was replaced with the BRBV counterpart (Fig. 1A), and the rescued virus showed a *ts* phenotype in cell culture (Fig. 2) and lost its replication ability and virulence in pigs (Fig. 1B). By dissecting IRES domain 4s of FMDV and BRBV, we first located the determinant of *ts&att* phenotypes on the loop in subdomain K of IRES domain 4 (Fig. 4A to D and Fig. 3) and finally determined that substitution of nucleotide C with G at position 351 on the loop in subdomain K of domain 4 of IRES is responsible for the *ts&att* phenotypes of FMDV (Fig. 4E and F and Fig. 3B). Importantly, the IRES C351G mutants of FMDV are highly attenuated among two main susceptible animal species—pigs and cattle (Table 1). Due to their temperature sensitivity characteristics, we speculate that the FMDV mutants carrying the IRES C351G mutation should be attenuated for other susceptible cloven-hoofed animal species. Thus, our study might solve the problem of varied attenuation among susceptible animals encountered in previous studies (2, 3).

Another main obstacle to develop live-attenuated FMDV vaccines is the difficulty of obtaining viruses that are both attenuated and immunogenic (2, 3). Here, the immunoprotective effect of a C351G mutant was tested in natural host pigs. The pigs inoculated with 10^6 $TCID_{50}$ of rC351G did not show any clinical signs of disease, viremia, or virus shedding (Table 1) in contrast to the animals inoculated with wild-type virus that developed severe disease at a dose of 10^5 $TCID_{50}$/animal (Table 1). However, the animals inoculated with a single dose of rC351G produced a rapid and potent neutralizing antibody response (Table 1) and exhibited complete protection against a challenge with a heterologous FMDV strain (Table 2). Therefore, our study achieves a perfect balance between FMDV attenuation and immunogenicity maintenance, thus solving another problem encountered in research on FMDV live-attenuated vaccines (2, 3).

The main concern for a live-attenuated vaccine is the possibility of reversion to virulence, especially for FMDV because of its high variability and quasispecies characteristics. In the genetic stability studies of the rC351G mutant *in vitro* (Fig. 7) and *in vivo*, no reverse mutation of the C351G IRES in cultured cells or reversion to virulence in the natural host pigs was observed. The inoculated animals showed no viremia, no virus excretion, and no transmission to susceptible animals (Table 1), revealing that the replication of these *ts&att* strains is strictly restricted in the body, which greatly reduces the risk of virulence reversion *in vivo*. Unlike the C351G mutants of FMDV, the poliovirus vaccine strains that are neuroattenuated empirically and replicate selectively in the gut have a long shedding period and can be transmitted in the human population (34), which provides an opportunity for mutation recovery in Sabin strains and virulence reversion in inoculated children (34). Thus, our manipulation of the FMDV IRES, especially mutation of C351G, is a feasible strategy to develop safe FMDV attenuated strains. However, an extensive study is required to evaluate the safety of this type of FMDV attenuated strain, including the effects of higher dosages and more sensitive inoculation routes in susceptible animals and their safety in other natural hosts such as sheep, goats, and wild cloven-hoofed animals.

Due to the uncertainty of the critical virulence determinant and virulence attenuation mechanism of FMDV in natural host species, elucidating the molecular mechanism of virulence attenuation caused by the IRES C351G mutation is important for safe and effective evaluation of these *ts&att* strains. Furthermore, our studies revealed that the C351G mutation of IRES causes a temperature-dependent translation defect of FMDV (Fig. 5) by reducing the binding between the cellular PTB protein and the IRES (Fig. 6), resulting in temperature-sensitive attenuation of FMDV (Fig. 4 and 3). A key event that occurred in this process is the binding of PTB to the IRES, with the C351G mutation becoming temperature sensitive (Fig. 6), which caused the translation activity of the C351G IRES (Fig. 5A) and the replication ability of FMDV *ts&att* mutants (Fig. 5B and C) to become temperature controlled. Importantly, temperature-sensitive control of the PTB-C351G IRES interaction at the body temperatures of cattle and pigs reflects an ideal

condition for *ts&att* mutants to both fully attenuate and be highly immunogenic. In our view, the virulence attenuation of FMDV caused by the IRES C351G mutation is a consequence of the interaction between the mutated IRES and cellular PTB protein to generate a temperature-sensitive phenotype. Given that the IRES C351G mutation can confer the virulence attenuation of FMDV, the PTB protein may be a common host factor acting on virulence attenuation in all natural susceptible hosts of FMDV. As an RNA chaperone protein, the PTB can stabilize the structure of the IRES and help eIFs and ITAFs interact with the IRES to form a translation initiation complex (35). The nucleotide G does not have a side chain, while the nucleotide C has a "-CH_2-SH" side chain, which might play an important role in binding with the PTB. Since the C351G mutation does not affect the predicted secondary structure of the IRES (Fig. 3B), we speculated that the mutation affects correct folding of the IRES and the stability of its three-dimensional structure through increasing temperatures followed by decreasing PTB binding, thus affecting the formation of the translation initiation complex. This process is complex, and more elaborate mechanisms need to be elucidated in future studies.

In porcine-derived IBRS-2 cells (Fig. 4B and F), the *ts* phenotype of attenuated strain rC351G and avirulent strain FMDV(R4) is more obvious than in hamster-derived BHK-21 cells (Fig. 4A and E), although all of these mutants are highly attenuated in both mice and pigs (Fig. 1 and 3B and Table 1). The molecular basis for this replication difference of these virus mutants in different cell lines is not clear. Importantly, the replication capacity of rC351G and FMDV(R4) in hamster-derived BHK-21 cells did not change at 37°C, which is very valuable for the attenuated strains with the IRES C351G mutation as seed viruses of potential live vaccines and for the avirulent strain with IRES domain 4 replacement as a seed virus of an inactivated vaccine. One approach for safer inactivated vaccine manufacturing that does not require a high-containment facility for production is to replace the wild-type virus with the avirulent strain FMDV(R4), which can grow well in BHK-21 cell culture but does not replicate and cause disease in natural hosts. Notably, FMDV(R4) with IRES domain 4 replacement lost its replication ability in a host-derived IBRS-2 cell line (Fig. 4B) and its virulence in host pigs (Fig. 1B), but the rC351G mutant with an IRES point mutation was restrictedly replicative in the host-derived cell line (Fig. 4F) and highly attenuated in host pigs and cattle (Table 1). This difference between FMDV(R4) and rC351G in the ability to replicate in the cell line and hosts may be related to the entire replacement of viral IRES domain 4 versus the one point mutation of C351G in the IRES, which results in a greater effect on the IRES translation activity of FMDV through interactions with cellular ITAF(s) and/or eIF(s).

In summary, we found that the IRES is a critical virulence determinant of FMDV, and the molecular mechanisms for the *ts&att* phenotypes caused by the IRES C351G mutation were elucidated. In addition, the IRES C351G as a decisive mutation for virus virulence was demonstrated among three serotypes of FMDV strains (Fig. 8), and in a comparative analysis, the C351 site of the IRES was found to be absolutely conserved among all serotypes of FMDV strains available in GenBank. Thus, manipulation of the IRES has allowed us to derive safe and effective *ts&att* FMDV mutants by changing their interactions with IRES-specific *trans*-acting factor PTB for the development of potential live-attenuated FMDV vaccines. In addition, this strategy may be appropriate for the rational design of and research on live-attenuated vaccines for other RNA viruses with IRES elements, such as hepatitis C virus (HCV), enterovirus 71 (EV71), and bovine viral diarrhea virus (BVDV).

MATERIALS AND METHODS

Ethics statement. All animal experiments were performed in enhanced biosafety level 3 (P3+) containment facilities approved by the review board of the Harbin Veterinary Research Institute (HVRI), Chinese Academy of Agricultural Sciences (CAAS). This study was carried out in strict accordance with the Chinese regulations of laboratory animals—The Guidelines for the Care of Laboratory Animals (Ministry of Science and Technology of People's Republic of China)—and laboratory animal requirements of the environment and housing facilities (GB 14925-2010, National Laboratory Animal Standardization Technical Committee). Protocols for the animal studies were approved by the Committee on the Ethics of Animal Experiments of the HVRI, CAAS (protocol number 150312-01 for mice, 161029-06 for pigs, and 181201-03 for cattle).

TABLE 3 Primers used in this study

No.	Primer	Sequence (5′→3′)[a]
1	d4N-1-F	CGCAGATCTTAATACGACTCACTATAGGTTGAAAGGGGGCGTTAGGGTCTC
2	d4N-1-R	CTCGGGGTACCTGAAGGGCATCCTTAGGCTGTCACCAGTGGTTGAGTACCAGTATC
3	d4N-2-F	TGGTGACAGCCTAAGGATGCCCTTCAGGTACCCCGAGGTAACACGCGAC
4	d4N-2-R	GGCCTCCGGTCACCTATTCAGCTTAGACGTTTTTTAAACCAGGCGCTTTT
5	d4N-3-F	CGGAGGCCGGCACCTTTCCTTCGAACAACTGTCTTTAACC
6	d4N-3-R	GAGGATATCGCTAGCTTTGAAAACCAGTCGTTG
7	d4J-1-F	CGCAGATCTTAATACGACTCACTATAGGTTGAAAGGGGGCGTTAGGGTCTC
8	d4J-1-R	TTGTTACCCCGGGGTACCTGGAGGGCATCCTTAGCCTGTCACCAGT
9	d4J-2-F	CGCAGATCTTAATACGACTCACTATAGGTTGAAAGGGGGCGTTAGGGTCTC
10	d4J-2-R	TCCTCAGATCCCGGGGTGTCACTTGTTACCCCGGGGTACCT
11	d4J-3-F	CACCCGGGATCTGAGGAGGGGACTGGGGCTTCTTTAAAAGCG
12	d4J-3-R	GAGGATATCGCTAGCTTTGAAAACCAGTCGTTG
13	d4K-1-F	CGCAGATCTTAATACGACTCACTATAGGTTGAAAGGGGGCGTTAGGGTCTC
14	d4K-1-R	GCTTTTTAAACTACGTAAAGTAGTCCCCTTCTCAGATCCCGAGTGT
15	d4K-2-F	CTTTACGTAGTTTAAAAAGCTTCTACGCCTGAATAGGTGACC
16	d4K-2-R	GAGGATATCGCTAGCTTTGAAAACCAGTCGTTG
17	d4K-loop-F	CTCGGGATCTGAGAAGGGGACTGGGGCTTTTTACAAGCGCCTGGTTTAAAAAGCTTC
18	d4K-loop-R	GAAGCTTTTTAAACCAGGCGCTTGTAAAAAGCCCCAGTCCCCTTCTCAGATCCCGAG
19	d4K-stem-F	CACTCGGGATCTGAGAAGGGGACTACCTTTAAGTAGTTTAAAAAGCTTCTACGCCTG
20	d4K-stem-R	CAGGCGTAGAAGCTTTTTAAACTACTTAAAGGTAGTCCCCTTCTCAGATCCCGAGTG
21	C351G-F	CTCGGGATCTGAGAAGGGGACTGGGGCTT**G**TTTAAAAGCGCCTGGTTTAAAAAGCTTC
22	C351G-R	GAAGCTTTTTAAACCAGGCGCTTTTAAA**C**AAGCCCCAGTCCCCTTCTCAGATCCCGAG
23	C351A-F	CTCGGGATCTGAGAAGGGGACTGGGGCTT**A**TTTAAAAGCGCCTGGTTTAAAAAGCTTC
24	C351A-R	GAAGCTTTTTAAACCAGGCGCTTTTAAA**T**AAGCCCCAGTCCCCTTCTCAGATCCCGAG
25	Ins C351-F	CGGGATCTGAGAAGGGGACTAC**C**TTTACGTAGTTTAAAAAGCTTCTACGCCTGAATAG
26	Ins C351-R	CAGGCGTAGAAGCTTTTTAAACTACGTAAA**G**GTAGTCCCCTTCTCAGATCCCGAGTGT
27	Del C351-F	CTCGGGATCTGAGAAGGGGACTGGGGCTTTTTAAAAGCGCCTGGTTTAAAAAGCTTC
28	Del C351-R	GAAGCTTTTTAAACCAGGCGCTTTTAAAAAGCCCCAGTCCCCTTCTCAGATCCCGAG
29	A-C351G-F	CTCGGGATCTGAGAAGGGGACTGGGGCTT**G**TATAAAAGCGCCCAGTTTAAAAAGCTTC
30	A-C351G-R	GAAGCTTTTTAAACTGGGCGCTTTTATA**C**AAGCCCCAGTCCCCTTCTCAGATCCCGAG
31	Asia1-C351G-F	CTCGGGATCTGAGAAGGGGACCGGGACTT**G**TTTAAAAGTGCCCGGTTTAAAAAGCTTC
32	Asia1-C351G-R	GAAGCTTTTTAAACCGGGCACTTTTAAA**C**AAGTCCCGGTCCCCTTCTCAGATCCCGAG
33	IBRS-PTB-F	GTCGAATTCATGGACGGCATCGTCCCAGACATAGCAGT
34	IBRS-PTB-R	TTACTCGAGCTAGATGGTGGACTTGGAGAAAGACAC>

[a]The nucleotides that have been changed are underlined and in boldface font.

Cells, viruses, and antibodies. Baby hamster kidney (BHK-21; ATCC CCL-10) and porcine kidney (IBRS-2; ATCC CRL-1835) cell lines were maintained in Dulbecco's modified Eagle's medium (DMEM; Gibco) containing 10% fetal bovine serum (FBS; Gibco) and 2 mM L-glutamine at 37°C in 5% CO_2. FMDV O/YS/CHA/05 (HM008917) was generated from the full-length infectious cDNA clone pYS (36), Asia1/YS/CHA/05 (GU931682) was derived from the full-length infectious cDNA clone pAsi (37), and A/QSA/CHA/2009, which shares 97.6% nucleotide sequence identity with A/HuBWH/CHA/2009 (JF792355) for the VP1 gene, was generated from the full-length infectious cDNA clone pQSA. FMDV O/CHA/2001 was derived from the full-length infectious cDNA clone pO01, which shares 99.4% identity with the complete genome sequence of FMDV O/CHA/99 (AJ539138). The O/M98/CHA/2010 strain was used as a challenge virus, which belongs to the Mya98 lineage of the O/SEA topotype and shares high levels of homology with subtype strain O/BY/CHA/2010 (JN998085). The chimeric-IRES FMDV mutants FMDV(R2), FMDV(R3), FMDV(R4), FMDV(R5), FMDV(RM,) and FMDV(BRBV) used in this study were constructed as described in a previous report (25). The monoclonal antibody (MAb) 4B2, which recognizes a conserved linear epitope on the VP2 protein of FMDV, was produced as described previously (38). Mouse anti-β-actin MAb (GenScript), mouse anti-glutathione *S*-transferase (GST) MAb (GenScript), mouse anti-PTB MAb (Novus Biological), and IRDye 800CW goat anti-mouse antibody (LI-COR) were used for Western blot detection.

Construction of IRES-chimeric FMDV infectious clone plasmids. Recombinant FMDV infectious cDNA clone plasmids with different chimeric IRESs were constructed using a BglII (nucleotide 1) and NheI (nucleotide 1949) cloning cassette to exchange the cognate IRES of FMDV with that of BRBV (NC_010354.1). The genetic structure of the cloning cassette in the pYS plasmid is as follows: BglII-T7 promoter, 5′ untranscribed region (UTR), L protein, and part of VP4-NheI. The primers used to construct these recombinant plasmids are listed in Table 3.

To construct pdN, the primer pairs 1 and 2, 3 and 4, and 5 and 6 were used to amplify DNA fragments of the FMDV 5′ terminus to the BRBV IRES subdomain N obtained from pFMDV(R4), FMDV IRES subdomains J to K obtained from pYS, and BRBV IRES subdomain N to FMDV VP4-NheI obtained from pFMDV(R4), respectively. The resulting PCR products were used as the templates to amplify overlapping products using the primer pair 1 and 6. Similarly, pdJ was constructed by amplifying the FMDV 5′ terminus to the IRES subdomain N obtained from pYS, BRBV IRES subdomain J obtained from pFMDV(R4), and FMDV IRES subdomain K to VP4-NheI obtained from pYS using primer pairs 7 and 8, 9 and 10, and 11 and 12, respectively, with subsequent fusion using the primer pair 7 and 12. For pdK, the primer pair

13 and 14 was used to amplify a PCR fragment encompassing the FMDV 5′ terminus to the IRES subdomain J obtained from pYS; this fragment was ligated to the PCR fragment corresponding to BRBV IRES subdomain K and FMDV IRES subdomain N to VP4-NheI obtained from pYS using primers 15 and 16.

For construction of the plasmids pK(loop), pK(stem), pC351G, pC351A, pIns-C351, pDel-C351, pA-C351G, and pAsia1-C351G, the FMDV infectious cDNA clone plasmid pYS, pAsi, or pQSA was digested with BglII/NheI, SphI/NdeI, or SpeI/NruI, respectively, and the resulting fragments were ligated into a pOK12 vector that was digested with corresponding restriction endonucleases. The resulting plasmids containing the IRESs from different serotypes of FMDV were used as the templates for site-directed mutagenesis. The primers (17 to 32) used to introduce the specific mutations are shown in Table 3. Mutagenesis was conducted using a QuikChange II site-directed mutagenesis kit (Stratagene). The mutated fragments were digested with BglII/NheI, SphI/NdeI, or SpeI/NruI and reintroduced into pYS, pAsi, or pQSA, respectively. The recombinant plasmid pO01-rC351G with the IRES C351G mutation was constructed using an infectious clone of pO01 as the backbone. The constructed recombinant plasmids were sequenced to confirm the introduced mutations and the absence of other changes.

***In vitro* transcription and transfection.** Plasmids were linearized by digestion with EcoRV (TaKaRa), and transcripts were generated using a RiboMAX Large Scale RNA Production Systems-T7 kit (Promega). After transcription, the reaction mixture was treated with 1 U of RQI DNase/μg RNA (Promega), and the transcript RNA was transfected into BHK-21 cells using Effectene transfection reagent (Qiagen). The recovered viruses were serially passaged five times in BHK-21 cells and stored at −70°C. Viral full-length genomes were sequenced, and viral titers were determined by $TCID_{50}$ assays as described previously (39).

Growth curves of FMDV at different temperatures. To determine viral replication kinetics, growth experiments in BHK-21 and IBRS-2 cells were carried out as follows. Cell monolayers in 6-well tissue culture plates were washed with phosphate-buffered saline (PBS) and inoculated with the virus at a multiplicity of infection (MOI) of 0.05. The plates were incubated for 1 h at 37°C, and the cells were thoroughly washed to remove unbound virus and placed at 33°C, 37°C, or 41°C. At 0, 4, 8, 16, 24, 32, and 40 h postinfection, the dishes were subjected to three consecutive freeze-thaw cycles, and the viral titers of the supernatants were determined by $TCID_{50}$ assay.

Western blotting. Western blotting was performed as described previously (25). Protein samples were separated by 12% SDS-PAGE and transferred to a polyvinylidene difluoride (PVDF) membrane. The membrane was blocked with 5% skim milk in PBS and then incubated with primary antibodies followed by the secondary antibody IRDye 800CW goat anti-mouse IgG, and signal detection was performed using a near-infrared fluorescence scanning imaging system (LI-COR Odyssey).

Construction of FMDV dual-luciferase reporters and luciferase assay. The dual-luciferase reporter plasmids containing the wild-type and mutant FMDV IRES were constructed as follows: the *Renilla* luciferase gene (RLuc) was amplified from a pRL-TK vector (Promega) and cloned into the SacI and MluI sites of the pGL3-Basic vector (Promega), which contains the firefly luciferase gene (FLuc). The resulting plasmid pRHF was further inserted with a fragment of the wild-type IRES or C351G mutation IRES between RLuc and FLuc through BglII and NcoI sites and named pRHF-IRES(WT) or pRHF-IRES(C351G), respectively. Then, a pVAX1 vector (Invitrogen) containing a cytomegalovirus (CMV) promoter was amplified with EcoRI and BamHI sites and ligated with a fragment of RLuc-IRES-FLuc that amplified from the construct pRHF-IRES(WT) or pRHF-IRES(C351G); the dual-luciferase reporter plasmid was named pCMV-RHF-IRES(WT) or pCMV-RHF-IRES(C351G), respectively. Next, these two dual-luciferase reporter plasmids were transfected into monolayers of BHK-21 cells or IBRS-2 cells in 6-well plates using Effectene transfection reagent (Qiagen) for incubation at 33°C, 37°C, or 41°C in DMEM with 2% FBS. At 24 h posttransfection, the activity of the RLuc and FLuc reporter genes was measured using a Dual-luciferase reporter assay kit (Promega). As the expression of RLuc is driven by the CMV promoter while the expression of FLuc is dependent on FMDV IRES activity, the ratio of the FLuc expression level to the RLuc expression level represents the relative translation efficiency of the FMDV IRES in a sample.

Expression and purification of PTB. The gene encoding PTB was PCR-amplified from IBRS-2 cells with the primer pair 33 and 34 (Table 3) and cloned into the plasmid pGEX-6P-1 (Novagen). A correct recombinant plasmid was transformed into competent cells of *Escherichia coli* Rosetta (DE3) pLys-S (Invitrogen), and a transformant was cultured by the addition of 0.1 mM isopropyl β-D-thio-galactopyranoside (IPTG) for induction of protein expression at 25°C for 16 h. GST-fused PTB protein was then purified with glutathione resin and a GST Fusion Protein purification kit (GenScript) according to the recommendations of the manufacturer.

Construction of a stable cell line overexpressing PTB. The PCR-amplified PTB gene from IBRS-2 cells was ligated into the pLVX-IRES-ZsGreen1 retroviral vector (Clontech), resulting in a recombinant plasmid—pLVX-ZsGreen1-PTB. HEK293T cells were cotransfected with 10.5 μg of pLVX-ZsGreen1-PTB in combination with 7 μg of psPAX2 (a packaging plasmid) and 3.5 μg of pMD2.G (an envelope plasmid) (Addgene), and pLVX-IRES-ZsGreen1 was used as a control. At 6 h posttransfection, the medium was replaced with fresh DMEM containing 5% FBS. After 48 h of incubation, the supernatant was filtered through a 0.22-μm membrane. The filtrates were ultracentrifuged to concentrate the recombinant lentivirus expressing ZsGreen1-PTB (Lenti-ZsGreen1-PTB) or wild-type lentivirus expressing ZsGreen1 (Lenti-ZsGreen1). Subsequently, IBRS-2 cells were transduced with lentiviruses at 10 transduction units (TUs) per cell, and the transduced cells expressing ZsGreen1-PTB or ZsGreen1 were examined by flow cytometry on a MoFlo XDP high-speed cell sorter (Beckman Coulter) and by Western blotting. The cell lines that consistently expressed ZsGreen1-PTB or ZsGreen1 were purified by limited dilution, proliferated, and named IBRS-2^{PTB} or IBRS-$2^{ZsGreen}$, respectively.

Biotinylated RNA pulldown assay. The plasmid pVAX1 (Invitrogen) was used to clone the full-length FMDV IRES and its mutant form (C351G). The constructed plasmids were linearized with EcoRV

and purified by phenol-chloroform extraction. A total of 2 μg of the linearized plasmid DNA was transcribed *in vitro* into RNA using the RiboMAX Large Scale RNA Production Systems-T7 kit (Promega) and purified with a MEGA Clear kit (Ambion) according to the manufacturer's protocol. For RNA labeling, the RNA was synthesized in a 20-μl transcription reaction mixture by adding 1.25 μl of 20 mM biotin-16-UTP (Roche). The biotinylated RNA was heated to 90°C for 2 min in RNA folding buffer (10 mM Tris [pH 7], 0.1 M KCl, and 10 mM $MgCl_2$), and the mixture was shifted to room temperature for 20 min to allow proper secondary structure formation. For the biotinylated RNA binding assay, a reaction mixture containing 100 μg of purified PTB from *E. coli* expression and 5 μg of biotinylated RNA was prepared. The mixture, at a final volume of 100 μl, was incubated in RNA mobility shift buffer (5 mM HEPES [pH 7.1], 40 mM KCl, 2 mM $MgCl_2$, 1 U RNasin, and 0.25 mg/ml heparin) for 60 min at 33°C, 37°C, or 41°C and then added to 100 μl of Dynabeads M 280 streptavidin (Invitrogen) for 10 min at room temperature. The RNA protein complexes were washed five times with RNA mobility shift buffer without heparin. After the last wash, 30 μl of 1$\times$ SDS-PAGE sample buffer was added to the beads, and the bound PTB protein was subjected to Western blot analysis.

Binding affinity measurement. Biolayer interferometry was performed to quantitatively detect the interaction between the FMDV IRES and PTB using an Octet Red 96 instrument (ForteBio Inc.). The experiment consisted of six steps, including baseline acquisition, biotinylated RNA loading onto the sensor, a second baseline acquisition, association of PTB purified from *E. coli* for measurement of K_{on}, dissociation of PTB for measurement of K_{dis}, and calculation of the equilibrium dissociation constant (K_D) by the ratio of K_{dis} to K_{on}. Specifically, the biotinylated FMDV IRES or its mutant at 500 nM was loaded onto streptavidin-coated biosensors and incubated with PTB. Five concentrations of PTB ranging from 48.75 to 780 nM were used for detection. The binding data were collected at 33°C, 37°C, and 41°C.

Pathogenicity testing of FMDV mutants in suckling mice. Three-day-old BALB/c suckling mice were divided randomly into different experimental groups, with 6 to 10 mice per group. The suckling mice were cervicodorsally inoculated with 100 μl of 10-fold serial dilutions containing FMDV mutants between 10^7 and 10^{-2} $TCID_{50}$ as described previously (40, 41), and FMDV(WT) was used as a control. Dead mice were scored up to 7 days after inoculation, and the 50% lethal dose (LD_{50}) was determined by the method of Reed and Muench (42).

Pathogenicity testing of FMDV mutants in pigs. The selected FMDV mutants, FMDV(R4) and rC351G, were tested for their virulence in pigs. Briefly, different groups of 2-month-old Yorkshire-cross pigs (15 to 20 kg) were housed in a single room for 1 week of acclimation. Prior to infection, the animals were moved to separate rooms. Each group of three pigs was i.m. inoculated with either 10^6 $TCID_{50}$ of FMDV(R4), 10^6 $TCID_{50}$ of rC351G, or 10^5 $TCID_{50}$ of FMDV(WT), and after 24 h, two naive pigs were added to each of the groups for direct contact. Sera and nasal/oral secretions were collected daily for up to 7 dpi and once a week thereafter. All animals underwent a clinical evaluation, and rectal temperature was measured daily throughout the experiment. Clinical scoring was performed based on the presence of vesicles in the mouth and on the feet, with a maximum score of 20 as described previously (43). FMDV RNA in sera and swab samples was measured by real-time reverse transcription-PCR (RT-PCR) as described below.

Pathogenicity testing of an FMDV mutant in cattle. Three steers (200 to 250 kg) were intradermally inoculated at multiple sites on the tongue with either 10^7 $TCID_{50}$ of O01-WT/animal or 10^7 $TCID_{50}$ of O01-rC351G/animal in different animal rooms, and 24 h later, two naive steers were added to the O01-rC351G-inoculated group for direct contact. Rectal temperature measurements and clinical exams with sedation to identify secondary site replication (vesicles) were performed daily. Clinical scoring based on the presence of vesicles in the mouth and on the feet (with a maximum score of 20) was performed as previously described (44). The samples collected consisted of sera and nasal and oral swabs collected daily up to 10 dpi and at 14 dpi. FMDV RNA was measured in sera and swab samples by real-time RT-PCR as described below.

Vaccination and challenge of pigs. Three 2-month-old pigs (15 to 20 kg) were i.m. vaccinated with the FMDV mutant rC351G (10^6 $TCID_{50}$/animal) followed by a challenge at 21 days postvaccination (dpv) with 1,000 pig median infected dose (PID_{50}) of virulent FMDV O/M98/CHA/2010/animal i.m. inoculated in the neck. Two additional pigs were inoculated with PBS as challenge controls. After the challenge, clinical signs were monitored daily during the first week, and samples were collected for detection of viral RNA and antibodies.

***In vitro* and *in vivo* passaging of an FMDV mutant.** The FMDV mutant rC351G was serially passaged 20 times in BHK-21 cells to assess its genetic stability *in vitro*. BHK-21 cells were infected with rC351G (MOI of 0.1) and incubated at 37°C until the appearance of a CPE. At the 20th blind passage, viral RNA was extracted as a template for RT-PCR, and the purified PCR amplicons were directly used for sequencing.

rC351G was also serially passaged in pigs three times to identify its genetic stability during pig-to-pig passages. Nine 2-month-old pigs (15 to 20 kg) were randomly divided into three groups for treatment with rC351G. For the first passage (P1), three pigs were i.m. injected with 10^6 $TCID_{50}$ of rC351G. At 5 dpi, all P1 pigs were euthanized for necropsy. Mixtures prepared from the tonsils, sera, and oral/nasal secretions of P1 pigs were homogenized and inoculated into P2 pigs for subsequent passaging. A homogenized mixture of tissue from inoculated P2 pigs was inoculated into P3 pigs for the last passage. The pigs used for passaging were observed daily for clinical signs. Sera and nasal and oral swab samples were collected daily for detection of viral RNA and antibodies.

Real-time RT-PCR for the detection of FMDV RNA. Real-time RT-PCR (rRT-PCR) detection of FMDV RNA was performed as described previously (45). RNA copy numbers per milliliter of fluid in sera and swab samples were calculated based on an O/YS/CHA/05-specific or O/CHA/2001-specific calibration

curve developed with *in vitro*-synthesized RNA obtained from pYS or pO01, respectively. For this procedure, a known amount of FMDV RNA was 10-fold serially diluted in nuclease-free water, and each dilution was tested in triplicates by rRT-PCR. Threshold cycle (C_T) values from triplicates were averaged and plotted against the FMDV RNA copy number; $10^{2.6}$ RNA copies/ml from preclinical samples (sera and swabs) was considered the cutoff value.

Microneutralization assay. Serum samples from all pigs or cattle were tested for the presence of FMDV-specific neutralizing antibodies by a microneutralization assay according to the Office International des Epizooties (OIE) manual (http://www.oie.int/fileadmin/Home/eng/Animal_Health_in_the_World/docs/pdf/2.01.05_FMD.pdf).

Indirect ELISA for detection of 3ABC antibodies. An indirect enzyme-linked immunosorbent assay (ELISA) kit (Lanzhou Veterinary Research Institute, Lanzhou, China) was used for the detection of FMDV 3ABC antibodies as described previously (46), and the titer of 3ABC antibodies was expressed as the ratio of the test to the positive control. In this assay, a cutoff value of 0.2 was recommended to distinguish between vaccinated and infected animals.

Statistical analysis. Data processing and analysis and graphic representation were performed using Prism (version 5.0) software (GraphPad Software, San Diego, CA). Statistical differences were determined using Student's *t* test. *P* values of >0.05 were considered not significant (NS).

ACKNOWLEDGMENTS

We thank Encarna Martinez-Salas from the Center of Molecular Biology Severo Ochoa, Spain, and Bindong Liu from the Meharry Medical College, USA, for critically reading and revising the manuscript and providing very helpful comments and suggestions.

This research was supported by the National Natural Science Foundation of China (grant no. 31770173 and 31400138) and the National Key Research and Development Program of China (grant no. 2016YFD0501505).

REFERENCES

1. Grubman MJ, Baxt B. 2004. Foot-and-mouth disease. Clin Microbiol Rev 17:465–493. https://doi.org/10.1128/cmr.17.2.465-493.2004.
2. Rodriguez LL, Grubman MJ. 2009. Foot and mouth disease virus vaccines. Vaccine 27(Suppl 4):D90–D94. https://doi.org/10.1016/j.vaccine.2009.08.039.
3. Diaz-San Segundo F, Medina GN, Stenfeldt C, Arzt J, de Los Santos T. 2017. Foot-and-mouth disease vaccines. Vet Microbiol 206:102–112. https://doi.org/10.1016/j.vetmic.2016.12.018.
4. Forattini OP. 1988. Smallpox, eradication and infectious diseases. Rev Saude Publica 22:371–374. (In Portuguese.) https://doi.org/10.1590/s0034-89101988000500001.
5. Normile D. 2008. Rinderpest. Driven to extinction. Science 319:1606–1609. https://doi.org/10.1126/science.319.5870.1606.
6. Minor PD. 2012. The polio-eradication programme and issues of the end game. J Gen Virol 93:457–474. https://doi.org/10.1099/vir.0.036988-0.
7. Moss WJ, Strebel P. 2011. Biological feasibility of measles eradication. J Infect Dis 204(Suppl 1):S47–S53. https://doi.org/10.1093/infdis/jir065.
8. Bachrach HL. 1968. Large-scale cultivation of animal cells in roller bottles for production of decigram amounts of pure foot-and-mouth disease virus. Natl Cancer Inst Monogr 29:73–79.
9. Brooksby JB. 1982. Portraits of viruses: foot-and-mouth disease virus. Intervirology 18:1–23. https://doi.org/10.1159/000149299.
10. Brown CC, Piccone ME, Mason PW, McKenna TS, Grubman MJ. 1996. Pathogenesis of wild-type and leaderless foot-and-mouth disease virus in cattle. J Virol 70:5638–5641. https://doi.org/10.1128/JVI.70.8.5638-5641.1996.
11. Piccone ME, Pacheco JM, Pauszek SJ, Kramer E, Rieder E, Borca MV, Rodriguez LL. 2010. The region between the two polyprotein initiation codons of foot-and-mouth disease virus is critical for virulence in cattle. Virology 396:152–159. https://doi.org/10.1016/j.virol.2009.10.020.
12. Uddowla S, Pacheco JM, Larson C, Bishop E, Rodriguez LL, Rai DK, Arzt J, Rieder E. 2013. Characterization of a chimeric foot-and-mouth disease virus bearing a bovine rhinitis B virus leader proteinase. Virology 447:172–180. https://doi.org/10.1016/j.virol.2013.08.035.
13. Segundo FD-S, Weiss M, Pérez-Martín E, Dias CC, Grubman MJ, Santos T. d l. 2012. Inoculation of swine with foot-and-mouth disease SAP-mutant virus induces early protection against disease. J Virol 86:1316–1327. https://doi.org/10.1128/JVI.05941-11.
14. Pacheco JM, Gladue DP, Holinka LG, Arzt J, Bishop E, Smoliga G, Pauszek SJ, Bracht AJ, O'Donnell V, Fernandez-Sainz I, Fletcher P, Piccone ME, Rodriguez LL, Borca MV. 2013. A partial deletion in non-structural protein 3A can attenuate foot-and-mouth disease virus in cattle. Virology 446:260–267. https://doi.org/10.1016/j.virol.2013.08.003.
15. Zeng J, Wang H, Xie X, Li C, Zhou G, Yang D, Yu L. 2014. Ribavirin-resistant variants of foot-and-mouth disease virus: the effect of restricted quasispecies diversity on viral virulence. J Virol 88:4008–4020. https://doi.org/10.1128/JVI.03594-13.
16. Rai DK, Diaz-San Segundo F, Campagnola G, Keith A, Schafer EA, Kloc A, de Los Santos T, Peersen O, Rieder E. 2017. Attenuation of foot-and-mouth disease virus by engineered viral polymerase fidelity. J Virol 91:e00081-17. https://doi.org/10.1128/JVI.00081-17.
17. Xie X, Wang H, Zeng J, Li C, Zhou G, Yang D, Yu L. 2014. Foot-and-mouth disease virus low-fidelity polymerase mutants are attenuated. Arch Virol 159:2641–2650. https://doi.org/10.1007/s00705-014-2126-z.
18. Martinez-Salas E, Francisco-Velilla R, Fernandez-Chamorro J, Lozano G, Diaz-Toledano R. 2015. Picornavirus IRES elements: RNA structure and host protein interactions. Virus Res 206:62–73. https://doi.org/10.1016/j.virusres.2015.01.012.
19. Ochs K, Zeller A, Saleh L, Bassili G, Song Y, Sonntag A, Niepmann M. 2003. Impaired binding of standard initiation factors mediates poliovirus translation attenuation. J Virol 77:115–122. https://doi.org/10.1128/jvi.77.1.115-122.2003.
20. De Quinto SL, Martínez-Salas E. 2000. Interaction of the eIF4G initiation factor with the aphthovirus IRES is essential for internal translation initiation *in vivo*. RNA 6:1380–1392. https://doi.org/10.1017/S1355838200000753.
21. Hellen CU, Witherell GW, Schmid M, Shin SH, Pestova TV, Gil A, Wimmer E. 1993. A cytoplasmic 57-kDa protein that is required for translation of picornavirus RNA by internal ribosomal entry is identical to the nuclear pyrimidine tract-binding protein. Proc Natl Acad Sci U S A 90:7642–7646. https://doi.org/10.1073/pnas.90.16.7642.
22. Luz N, Beck E. 1991. Interaction of a cellular 57-kilodalton protein with the internal translation initiation site of foot-and-mouth disease virus. J Virol 65:6486–6494. https://doi.org/10.1128/JVI.65.12.6486-6494.1991.
23. Komar AA, Hatzoglou M. 2015. Exploring internal ribosome entry sites as therapeutic targets. Front Oncol 5:233. https://doi.org/10.3389/fonc.2015.00233.
24. Lee KM, Chen CJ, Shih SR. 2017. Regulation mechanisms of viral IRES-driven translation. Trends Microbiol 25:546–561. https://doi.org/10.1016/j.tim.2017.01.010.
25. Sun C, Yang D, Gao R, Liang T, Wang H, Zhou G, Yu L. 2016. Modification of the internal ribosome entry site element impairs the growth of

foot-and-mouth disease virus in porcine-derived cells. J Gen Virol 97:901–911. https://doi.org/10.1099/jgv.0.000406.
26. Betts AO, Edington N, Jennings AR, Reed SE. 1971. Studies on a rhinovirus (EC11) derived from a calf. II. Disease in calves. J Comp Pathol 81:41–48. https://doi.org/10.1016/0021-9975(71)90053-3.
27. Lozano G, Martinez-Salas E. 2015. Structural insights into viral IRES-dependent translation mechanisms. Curr Opin Virol 12:113–120. https://doi.org/10.1016/j.coviro.2015.04.008.
28. Kolupaeva VG, Hellen CU, Shatsky IN. 1996. Structural analysis of the interaction of the pyrimidine tract-binding protein with the internal ribosomal entry site of encephalomyocarditis virus and foot-and-mouth disease virus RNAs. RNA 2:1199–1212.
29. Pineiro D, Fernandez N, Ramajo J, Martinez-Salas E. 2013. Gemin5 promotes IRES interaction and translation control through its C-terminal region. Nucleic Acids Res 41:1017–1028. https://doi.org/10.1093/nar/gks1212.
30. Domingo E, Escarmis C, Martinez MA, Martinez-Salas E, Mateu MG. 1992. Foot-and-mouth disease virus populations are quasispecies. Curr Top Microbiol Immunol 176:33–47. https://doi.org/10.1007/978-3-642-77011-1_3.
31. Yuan T, Wang H, Li C, Yang D, Zhou G, Yu L. 2017. T135I substitution in the nonstructural protein 2C enhances foot-and-mouth disease virus replication. Virus Genes 53:840–847. https://doi.org/10.1007/s11262-017-1480-9.
32. Alexandersen S, Mowat N. 2005. Foot-and-mouth disease: host range and pathogenesis. Curr Top Microbiol Immunol 288:9–42. https://doi.org/10.1007/3-540-27109-0_2.
33. Hollister JR, Vagnozzi A, Knowles NJ, Rieder E. 2008. Molecular and phylogenetic analyses of bovine rhinovirus type 2 shows it is closely related to foot-and-mouth disease virus. Virology 373:411–425. https://doi.org/10.1016/j.virol.2007.12.019.
34. Minor PD. 2015. Live attenuated vaccines: historical successes and current challenges. Virology 479–480:379–392. https://doi.org/10.1016/j.virol.2015.03.032.
35. Song Y, Tzima E, Ochs K, Bassili G, Trusheim H, Linder M, Preissner KT, Niepmann M. 2005. Evidence for an RNA chaperone function of polypyrimidine tract-binding protein in picornavirus translation. RNA 11:1809–1824. https://doi.org/10.1261/rna.7430405.
36. Liang T, Yang D, Liu M, Sun C, Wang F, Wang J, Wang H, Song S, Zhou G, Yu L. 2014. Selection and characterization of an acid-resistant mutant of serotype O foot-and-mouth disease virus. Arch Virol 159:657–667. https://doi.org/10.1007/s00705-013-1872-7.
37. Wang H, Zhao L, Li W, Zhou G, Yu L. 2011. Identification of a conformational epitope on the VP1 G-H Loop of type Asia1 foot-and-mouth disease virus defined by a protective monoclonal antibody. Vet Microbiol 148:189–199. https://doi.org/10.1016/j.vetmic.2010.09.013.
38. Yu Y, Wang H, Zhao L, Zhang C, Jiang Z, Yu L. 2011. Fine mapping of a foot-and-mouth disease virus epitope recognized by serotype-independent monoclonal antibody 4B2. J Microbiol 49:94–101. https://doi.org/10.1007/s12275-011-0134-1.
39. Pizzi M. 1950. Sampling variation of the fifty percent end-point, determined by the Reed-Muench (Behrens) method. Hum Biol 22:151–190.
40. Baranowski E, Molina N, Nunez JI, Sobrino F, Saiz M. 2003. Recovery of infectious foot-and-mouth disease virus from suckling mice after direct inoculation with *in vitro*-transcribed RNA. J Virol 77:11290–11295. https://doi.org/10.1128/jvi.77.20.11290-11295.2003.
41. Gutiérrez-Rivas M, Pulido MR, Baranowski E, Sobrino F, Sáiz M. 2008. Tolerance to mutations in the foot-and-mouth disease virus integrin-binding RGD region is different in cultured cells and *in vivo* and depends on the capsid sequence context. J Gen Virol 89:2531–2539. https://doi.org/10.1099/vir.0.2008/003194-0.
42. Reed LJ, Muench H. 1938. A simple method of estimating fifty per cent endpoints. Am J Hyg 27:493–497.
43. Pacheco JM, Mason PW. 2010. Evaluation of infectivity and transmission of different Asian foot-and-mouth disease viruses in swine. J Vet Sci 11:133–142. https://doi.org/10.4142/jvs.2010.11.2.133.
44. Pacheco JM, Arzt J, Rodriguez LL. 2010. Early events in the pathogenesis of foot-and-mouth disease in cattle after controlled aerosol exposure. Vet J 183:46–53. https://doi.org/10.1016/j.tvjl.2008.08.023.
45. Shaw AE, Reid SM, Ebert K, Hutchings GH, Ferris NP, King DP. 2007. Implementation of a one-step real-time RT-PCR protocol for diagnosis of foot-and-mouth disease. J Virol Methods 143:81–85. https://doi.org/10.1016/j.jviromet.2007.02.009.
46. Lu Z, Cao Y, Guo J, Qi S, Li D, Zhang Q, Ma J, Chang H, Liu Z, Liu X, Xie Q. 2007. Development and validation of a 3ABC indirect ELISA for differentiation of foot-and-mouth disease virus infected from vaccinated animals. Vet Microbiol 125:157–169. https://doi.org/10.1016/j.vetmic.2007.05.017.
47. Zuker M. 2003. Mfold web server for nucleic acid folding and hybridization prediction. Nucleic Acids Res 31:3406–3415. https://doi.org/10.1093/nar/gkg595.